

A COMPARATIVE STUDY OF VARIOUS DIGITAL MODULATION TECHNIQUES

**A Thesis Submitted
in Partial Fulfilment of the Requirements
for the Degree of
MASTER OF TECHNOLOGY**

By

Lt. A. K. TIWARI

**to the
DEPARTMENT OF ELECTRICAL ENGINEERING
INDIAN INSTITUTE OF TECHNOLOGY, KANPUR
AUGUST, 1981**

EE-1981-M-TIKI-COM

I.I.T. KANPUR
CENTRAL LIBRARY

Acc. No. **A 66972**

8 SEP 1981

CERTIFICATE

Certified that this work on "A COMPARATIVE STUDY OF VARIOUS DIGITAL MODULATION TECHNIQUES" has been carried out under my supervision and that this has not been submitted elsewhere for a degree.

KANPUR-16
August, 1981

Vishwanath Sinha
(Vishwanath Sinha)
Assistant Professor
Department of Electrical Engineering
Indian Institute of Technology
KANPUR

ACKNOWLEDGEMENT

I am greatly indebted to Dr. V. Sinha for suggesting this topic and providing valuable guidance to enable me to complete this work.

I take this opportunity to thank M/s Govind Sharma and P.G. Poonacha for their valuable help. Thanks are also due to Mr. J.S. Rawat who has done an excellent job of typing this thesis.

IIT Kanpur
Aug, 1981

(A.K. Tiwari)
Lt.
Indian Navy

LIST OF CONTENTS

	Page
LIST OF FIGURES	iv
LIST OF TABLES	vi
ABSTRACT	viii
CHAPTER 1 INTRODUCTION	1
CHAPTER 2 PERFORMANCE OF SYSTEMS UNDER IDEAL CONDITIONS	7
2.1 Introduction	7
2.2.1 On-Off Keying: Coherent Detection	8
2.2.2 On-Off Keying: Envelope Detection	9
2.3.1 Binary Frequency Shift Keying: Coherent Detection	10
2.3.2 Binary Frequency Shift Keying: Non-coherent detection	11
2.4.1 Binary Phase Shift Keying: Ideal Coherent Detection	11
2.4.2 Binary Phase Shift Keying: Differential Detection	12
2.5.1 Multiphase PSK: Coherent Detection	12
2.5.2 Multiphase PSK: Differential Detection	20
2.6 Minimum Shift Keying ($h=0.5$) and Offset Keyed QPSK Signaling	21
2.7.1 Continuous Phase FSK($h=0.715$): Coherent Detection	29
2.7.2 Continuous Phase FSK($h=0.715$): Non-Coherent Detection	39
2.8 Comparison of Modulation Schemes	49

	Page
CHAPTER 3 COMMUNICATION EFFICIENCY	52
3.1 Introduction	52
3.2 Multitone Frequency Shift Keying	52
3.3 Multiphase Phase Shift Keying	57
3.4 Linear Modulation	59
3.5 Results and Conclusions	61
CHAPTER 4 PERFORMANCE OF SYSTEMS UNDER RAYLEIGH FADING	74
4.1 Introduction	74
4.2.1 OOK: Non-coherent Detection	74
4.2.2 OOK: Coherent Detection	78
4.3.1 BFSK: Coherent Detection	79
4.3.2 BFSK: Non-coherent Detection	79
4.4.1 BPSK: Ideal Coherent Detection	80
4.4.2 DPSK	81
4.5 MSK ($h = 0.5$) and QPSK	81
4.6.1 Multiphase PSK: Coherent Detection	82
4.6.2 Multiphase PSK: Differential Detection	87
4.7 Comparison of Modulation Schemes	89
CHAPTER 5 PERFORMANCE OF SYSTEMS UNDER LINEAR DIVERSITY COMBINING TECHNIQUES	91
5.1 Introduction	91
5.2.1 BFSK: Coherent Detection	94
5.2.2 BFSK: Envelope Detection	97
5.3.1 BPSK: Ideal Coherent Detection	99

5.3.2 DPSK	101
5.4 OOK: Coherent Detection	102
5.5 Multiphase PSK: Coherent Detection	103
5.6 MSK and OK-QPSK Signalling	110
5.7 Comparison of Various Modulation Schemes	110
CHAPTER 6 CONCLUSIONS	115
REFERENCES	121
APPENDIX A	
APPENDIX B	

LIST OF FIGURES

Fig. No.		Page
2.1	M-phase Signaling (M=8)	15
2.2	Bounds for Errors in M-phase PSK	17
2.3	Block Diagram of CPFSK Coherent Receiver	32
2.4	Performance of CPFSK Coherent Receiver	36
2.5	Block diagram of CPFSK Non-coherent Receiver	42
2.6	Performance of CPFSK Non-coherent Receiver	47
3.1	Data Rate Comparison of Systems	65
3.2	Number of Levels Versus SNR for Various Systems	66
3.3	Bandwidth Expansion Factor B/N Versus Number of Optimum Levels	67
3.4	Bandwidth Expansion Factor B/N Versus SNR for Optimised FSK	68
3.5	Bits per Cycle R/B Versus SNR for Optimised FSK and differential PM at $P_e = 10^{-6}$	69
3.6	Bits per cycle R/B Versus SNR for Optimised FSK and Differential PM at $P_e = 10^{-8}$	70
4.1	Performance of Multiphase Coherent PSK under Rayleigh Fading	86

Fig. No.	Title	Page
5.1	Performance of FSK under Diversity	96
5.2	Performance of QPSK under Diversity	105
5.3	Performance of Multiphase Coherent PSK under Diversity	109
	Block Diagrams of Binary On-off Keyed Coherent and Envelope Detection Receivers	B1
	Block Diagrams of binary FSK Coherent and Non-coherent Receivers	B2
	Block Diagrams of Binary PSK Coherent and Differential Receivers	B3

LIST OF TABLES

	Page
Table 2.1 : Lower Bound on Probability of Error for CPFSK Coherent Detection	37
Table 2.2 : Upper Bound on Probability of Error for CPFSK Non-coherent Detection	38
Table 2.3 : Probability of Errors for BPSK and CPFSK Non-coherent Detection	46
Table 2.4 : Ideal Performance of Representative Modulation Schemes	50
Table 3.1 : Data Rates at Various SNRs for FSK Optimum Detection	62
Table 3.2 : Data Rates at Various SNRs for PSK Coherent Detection	62
Table 3.3 : Data Rates at Various SNRs for PSK Differential Detection	63
Table 3.4 : Data Rates at Various SNRs for SSB-SC AM	63
Table 3.5 : Data Rates at Various SNRs for DSB-SC AM	64
Table 4.1 : Probability of Error for Multiphase PSK Under Rayleigh Fading	85
Table 4.2 : Performance of Representative Schemes on Rayleigh Fading Channel	89
Table 5.1 : Probability of Errors at Various SNRs for FSK: Coherent Detection (under maximal ratio combining)	95
Table 5.2 : Probability of Errors at Various SNRs for FSK: Non-coherent Detection (under maximal ratio combining)	98

Table 5.3 :	Probability of Errors at Various SNRs for Differential PSK (under maximal ratio combining)	100
Table 5.4 :	Probability of Errors at Various SNRs for QPSK (under maximal ratio combining)	104
Table 5.5 :	Probability of Errors at Various SNRs for 8-phase PSK (under maximal ratio combining)	107
Table 5.6 :	Probability of Errors at Various SNRs for 16-phase PSK (under maximal ratio combining)	108
Table 5.7 :	Performance of Representative Digital Modulation Schemes under Maximal Ratio Combining (M=2)	111
Table 5.8 :	Performance of Representative Digital Modulation Schemes under Maximal Ratio Combining (M=4)	112

ABSTRACT

The thesis presents a comparative study of various digital modulation techniques. The criterion for comparison has been the signal to noise ratio (SNR) needed per bit to achieve different bit error rates (BERs). Probability of error expressions have been obtained for various digital modulation techniques assuming the channel to be ideal. The relative performances have been shown in tabular form. Typical systems that have been studied are: Binary On-Off Keying, Binary Phase Shift Keying, Multiphase PSK, Minimum Shift Keying, Offset Keyed 4 Phase PSK (OK-QPSK), and Continuous Phase Frequency Shift Keying with a modulation index of 0.715.

The communication efficiencies as measured by data rate per unit bandwidth for multilevel ASK, multiphase PSK and multitone FSK systems have been obtained again assuming the channel to be ideal. The relative performances of these systems have been shown graphically.

The above studies have also been carried out when the channel is a Rayleigh fading channel. To overcome the effect of fading, linear diversity combining techniques are utilised. We have obtained the probability of error expressions for various digital modulation systems under maximal ratio combining technique only. Tables have been prepared to portray the relative performance of these systems under dual and quadrature diversities.

CHAPTER 1

INTRODUCTION

Digital communication systems have an inherent advantage over analog systems. This is mainly due to their reliability and ease with which they can be implemented, especially with present day digital technology. In a communication system, the flow of signal from transmitter to receiver is restricted by noise and various other impairments introduced by the channel. To overcome the effect of these impairments, various kinds of digital modems (modulator/demodulator) are used. Modulator part of the modem converts the digital signal into an appropriate analog one and this signal is then transmitted after suitable frequency translation and power amplifications. The demodulator, in turn, makes a decision about the digital information transmitted based on the received waveform. The desire to get better and better performance led to the advent of various modulation/demodulation techniques. Our objective in this thesis is to discuss the performance of some of these techniques under additive white Gaussian noise and subsequently under Rayleigh fading. The systems chosen for our studies are,

1. Binary On-Off Keying (OOK): Coherent as well as envelope detection schemes.
2. Binary Frequency Shift Keying (FSK): Coherent and noncoherent detection schemes.
3. Binary Phase Shift Keying (BPSK): Coherent as well as differential detection schemes.
4. Multiphase FSK (M-ary PSK): Coherent as well as differential detection schemes.
5. Minimum Shift Keying (MSK), $h=0.5$: Coherent detection scheme.
6. Offset Keyed QPSK
7. Continuous phase FSK (CPFSK), $h=0.715$: Coherent as well as non-coherent detection schemes where h is modulation index.

First digital modulation/demodulation scheme to come on the scene was OOK. The probability of error performance of this scheme either with coherent or with envelope detection was found to be poor. In this scheme the amplitude of received waveform (signal plus noise) itself is compared with a threshold. The threshold depends on the random nature of noise and for better performance, the system requires

a large signal power. FSK coherent and non-coherent schemes overcome this problem to a great extent. But this system has a drawback in which it occupies a great deal of bandwidth. The next system to be proposed was BPSK with coherent detection which gave best possible probability of error performance under the then existing digital modulation techniques. However, this technique needed an exact carrier phase reference at the receiver for the coherent detection of the received waveform. Extraction of exact phase reference was always elusive from hardware considerations and hence this difficulty led to the advent of DPSK where the relative phase of two successive pulses are utilised for detection purposes instead of absolute phase of a particular pulse. The need to achieve greater information rate led to the advent of multiphase PSK [25] coherent detection scheme. Although this system provides a very good data rate per unit bandwidth (R/B) performance, it is a very complex system to implement due to phase coherency required at the receiver. However, this problem was overcome by differential detection of received waveform but the probability of error performance deteriorated in this case (multiphase PSK with differential detection) [1,25]. At this ^{time} OK-QPSK was

proposed which gives reasonably good R/B performance in addition to cancelling the effect of ISI to a great extent [7,14, 16]. In an analog system of communication, amplitude (modulated signals occupy least amount of bandwidth followed by PM and FM systems (in that order). So is not the case in digital modulation systems where FSK system with slight modification can occupy lesser bandwidth than ASK or PSK systems.

This fact was demonstrated with the advent of CPFSK systems. It is seen that if abrupt phase transitions at bit intervals could be avoided, then the spectral characteristics of a system could be improved considerably. This fact was utilised in the study of CPFSK systems. MSK is a particular case of CPFSK where the modulation index (h) is assumed to be 0.5. In addition to giving a very good R/B performance, it also gives a good probability of error performance [7,13,16,26]. It was observed that if h is chosen to be 0.715, then the CPFSK performance under coherent detection was optimum [24]. This scheme with 3 or 5 bits of observation interval can outperform BPSK coherent scheme [6,12]. The problem of exact carrier phase reference at the receiver led to non-coherent detection of CPFSK($h=0.715$) waveform. This system is relatively simple to implement.

CPFSK ($h=0.715$) systems gives best possible probability of error performance among the existing techniques in addition to exhibiting a very good spectral characteristics [26] .

In Chapter 2, we have compared the performances of various digital modulation techniques mentioned earlier. The performance criterion has been SNR per bit required to achieve various bit error rates (BERs). The probability of error expressions have been obtained for these techniques assuming the channel to be ideal (defined as linear, infinite bandwidth channel, corrupted by additive white Gaussian noise only). A table has been prepared to portray the relative performance of these digital systems. Basic receiver structures of various systems have been given in Appendix B1 to B3.

In Chapter 3, we discuss the relative communication efficiencies measured as data rate per unit bandwidth for multiphase PSK, multilevel ASK and multitone FSK systems. Relative performance of the systems has been tabulated numerically and graphical representations given.

We consider the effect of Rayleigh fading on the performance of various digital modulation techniques in

Chapter 4. A table has been prepared to indicate the relative performance of these systems under Rayleigh fading.

To combat the severe degradations caused by Rayleigh fading in the performances of these systems, linear diversity combining techniques have been studied (in Chapter 5). Specifically, only maximal ratio combining has been discussed. The relative performance of these systems has again been shown in tabular forms under dual and quadrature diversities respectively.

Finally we conclude our studies in Chapter 6 by giving a comparative statement of modulation techniques in order of their complexities and outlining the further scope of study in this field.

CHAPTER 2

PERFORMANCE OF SYSTEMS UNDER IDEAL CONDITIONS

2.1 INTRODUCTION:

In this chapter performances of various modulation techniques under ideal conditions have been discussed to obtain expressions for probability of errors. Specifically we assume that

1. The channel is an Additive white gaussian noisy (AWGN) channel.
2. There is no inter-symbol interference (ISI).
3. There is no delay distortion introduced to the signal by the channel.

A comparative study is thereafter taken. The criterion for the comparative study is the average signal-to-noise-ratio (SNR) required per bit to achieve a particular bit error rate (BER). Three BER's have been arbitrarily chosen e.g. 10^{-4} , 10^{-6} and 10^{-8} . These would be tolerable BERs in voice, video and accuracy data respectively. While considering M-ary signaling, the symbol error rates have been converted to bit error rates and also the symbol SNR to bit SNR for comparison purposes. The criterion used to convert the symbol error rates to bit error rates and symbol SNRs to bit SNRs in

this chapter has also been followed in all the other chapters of the thesis.

2.2.1 On-off Keying (OOK): Coherent detection [1]

Here the transmitted signal can be written as

$$s(t) = \begin{cases} u(t) \cos w_c t & : \text{'1' (Mark)} \\ 0 & : \text{'0' (Space)} \end{cases} ; 0 \leq t < T \quad (2.2.1)$$

where w_c is angular carrier frequency. In general for the sake of simplicity, the modulating signal is taken to be a square pulse but it can be any well defined wave shape. The basic receiver structure and the corresponding probability of error under a threshold 'b' is given as

$$P_e = \frac{1}{2} \left[1 - \frac{1}{2} \operatorname{erfc}(b_0 / \sqrt{2} - \sqrt{\gamma}) \right] + \frac{1}{4} \operatorname{erfc}(b_0 / \sqrt{2}) \quad (2.2.2)$$

where,

$$\operatorname{erfc}(x) = \frac{2}{\sqrt{\pi}} \int_x^{\infty} e^{-t^2} dt$$

$$b_0 = \frac{b}{\sqrt{N}} = \text{normalised threshold}$$

N = average power of the total output noise

$$= \frac{u^2}{2N} = \text{SNR}; \frac{u^2}{2} \text{ is the peak signal power.}$$

The expression (2.2.2) is true for a fixed threshold. The optimum threshold can be found out by differentiating (2.2.2) with respect to b_0 and equating it to zero. The optimum value, \hat{b}_0 , is given as

$$\hat{b}_0 = \sqrt{\gamma/2} \quad (2.2.3)$$

Using equation (2.2.3) in equation (2.2.2), one gets

$$P_e = \frac{1}{2} \operatorname{erfc} \left(\sqrt{\frac{\gamma}{2}} \right) \quad (2.2.4)$$

The above expression is valid for equiprobable signals only.

The values of SNRs needed for various probabilities of errors are given in Table 2.4.

2.2.2 OOK: Envelope detection [1]

The basic receiver structure and P_e has been calculated in [1]. Under a fixed threshold of 'b', P_e is given by

$$P_e = \frac{1}{2} \left[1 - Q(\sqrt{2\gamma}, b_0) \right] + \frac{1}{2} e^{-b_0^2/2} \quad (2.2.5)$$

where,

$Q(\alpha, \beta)$ = Marcum's Q function

$$= \int_{\beta}^{\infty} t \operatorname{Io}(\alpha t) e^{-\frac{t^2 + \alpha^2}{2}} dt \quad (2.2.6)$$

where $\operatorname{Io}(\cdot)$ = Modified bessel function of zero order.

Optimum threshold, \hat{b}_0 , is obtained from

$$I_0(\hat{b}_0 \sqrt{2\gamma}) e^{-\gamma} = 1 \text{ or } \gamma = \ln I_0(\hat{b}_0 \sqrt{2\gamma}) \quad (2.2.7)$$

A good approximation to equation (2.2.7) is given as

$$\hat{b}_0 = \sqrt{2 + \gamma/2} \quad (2.2.8)$$

At high SNRs and under the assumption of optimum threshold, P_e is given by

$$\begin{aligned} P_e &\approx \frac{1}{4} \operatorname{erfc}(\sqrt{\gamma/2}) + \frac{1}{2} e^{-\gamma/4} \\ &\approx \frac{1}{2} e^{-\gamma/4} \end{aligned} \quad (2.2.9)$$

The values of SNRs needed for various probabilities of errors are given in Table 2.4.

2.3.1 Binary Frequency Shift Keying (FSK): Coherent detection [1]

The transmitted signal is generally represented as

$$s(t) = \begin{cases} u(t) \cos w_1 t : 1 \\ u(t) \cos w_2 t : 0 \end{cases} ; 0 \leq t < T \quad (2.3.1)$$

Here w_1 and w_2 are two carrier angular frequencies

The corresponding probability of error expression is

$$P_e = \frac{1}{2} \operatorname{erfc}(\sqrt{\gamma/2}) \quad (2.3.2)$$

where,

γ = average SNR.

The values of SNRs needed for various probabilities of errors are shown in Table 2.4.

2.3.2 FSK: Non-coherent detection [1]

A pair of tone filters are used in non-coherent detection of FSK and the output of each filter is envelope detected. The probability of error is given by

$$P_e = 1/2 e^{-\gamma/2} \quad (2.3.3)$$

The values of SNRs needed for various probabilities of errors are given in Table 2.4.

2.4.1 Binary Phase Shift Keying (BPSK): Ideal coherent detection [1]

The optimum expression for transmitted signal can be put in the following form,

$$s(t) = \begin{cases} u(t) \cos w_c t : 1 \\ -u(t) \cos w_c t : 0 \end{cases} ; 0 \leq t < T \quad (2.4.1)$$

with the expression for probability of error as

$$P_e = \frac{1}{2} \text{erfc} (\sqrt{\gamma}) \quad (2.4.2)$$

The receiver structure is given in [1].

The SNRs needed for various probabilities of errors are given in Table 2.4.

2.4.2 BPSK: Differential detection (DPSK) [1]

It is not always possible to obtain and maintain a coherent phase reference at the receiver. In such cases, it may be possible to utilise phase comparison of successive pulses for detection purpose. Thus the information is conveyed by the phase transitions between the pulses rather than the absolute phases of the pulses. Therefore a 'Mark' ('1') transmission is synonymous with a phase shift of 0° between two successive pulses and a 'Space' ('0') transmission synonymous with a phase shift of 180° between the two successive pulses. Thus the two inputs to the detector are a current pulse and second one being the current pulse delayed by a bit duration, T . Under the above conditions, the probability of error expression is given by [1] as

$$P_e = \frac{1}{2} e^{-\gamma} \quad (2.4.3)$$

The values of SNRs needed for various probabilities of error are given in Table 2.4.

2.5.1 Multi-phase PSK (M-ary PSK): coherent detection [1]

The requirement of higher data rate per unit bandwidth led to the advent of M-ary PSK. To understand this, let us

consider 4 phase PSK signaling. In BFSK, the data is transmitted on 0° or 180° phase positions of the carrier. Thus with respect to coherent detection, a completely independent binary signaling can be achieved at the 90° - 270° phase positions of the carrier. One signal can be visualised as DSB-SC modulation by $\cos w_c t$ and the other as DSB-SC modulation by $\sin w_c t$. Assuming perfect phase reference at the receiver, coherent detection by a $\cos w_c t$ reference will retrieve the first signal along with the noise component in phase with it and coherent detection by a $\sin w_c t$ reference will retrieve the other signal plus the quadrature component of the noise. Thus, without altering the signaling bandwidth, information rate can be doubled. But cost is paid in terms of increased transmitted signal power. In fact to keep the error rate constant, the signal power must be doubled in case of 4-phase PSK as compared to BPSK.

It is not possible, any more, to transmit any additional binary PSK signals on any other phase axes without producing cross-talks with both the quadrature signals already described in 4- phase PSK case. Still one could conceive of higher level signaling using other suitable phase axes. The severe drawback of extending it to higher than $M=4$ is the degradation of the system performance due to correlations between various

phases. Besides requiring stringent conditions of exact phase recovery, such situations could also end up with higher probability of errors. Thus, though higher data rates could be achieved, if one wants to retain the same probability of error, then the power to be transmitted is to be increased besides having to design a very complex receiver.

4 phase PSK signaling waveform can be represented as

$$s(t) = a \cos w_c t + b \sin w_c t \quad (2.5.1)$$

where,

$$a = \pm 1$$

$$b = \pm 1$$

hence,

$$s(t) = \sqrt{2} \cos(w_c t + \theta) \quad (2.5.2)$$

where,

$$\theta = 45^\circ, 135^\circ, 225^\circ, 315^\circ.$$

Expression (2.5.2) can be extended to general M-ary signaling which can be represented as

$$s(t) = \sqrt{2S} \cos (w_c t + \theta) \quad (2.5.3)$$

where

S = total signal power received

and θ can take any value in the discrete set

$\frac{2\pi k}{M}$; $k = 0, 1, 2 \dots M-1$. Usually M is taken to be a power of 2 ($M=2^n$, n an integer). Figure 2.1 shows M -ary signaling phase positions.

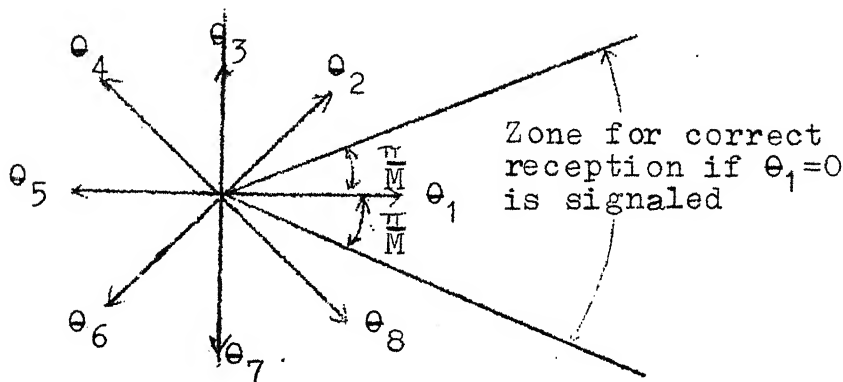


Figure 2.1: M-Phase Signaling ($M=8$)

An exact calculation of P_e is possible. But the ultimate result obtained is not easy for numerical evaluation. As our intention is to calculate SNRs required to achieve bit error rates of 10^{-4} and less, an approximate calculation of P_e is possible which is quite accurate for values of $M \geq 4$. It is also possible to calculate an exact expression in case of $M=4$ in a simple form. Thus we can use the approximate result to calculate SNR for $M=8$ and 16 only so that errors in calculation of SNRs at these values of M are insignificant.

The received signal can be written as (assuming $\theta = 0$ has been transmitted)

$$\begin{aligned} r(t) &= s(t) + n(t) \\ &= \sqrt{2S} \cos w_c t + x(t) \cos w_c t - y(t) \sin w_c t \\ &= [\sqrt{2S} + x(t)] \cos w_c t - y(t) \sin w_c t \end{aligned} \quad (2.5.4)$$

where the Gaussian noise $n(t)$ has been expressed by its inphase and quadrature components and

$$\overline{x^2} = \overline{y^2} = \overline{n^2} = N$$

Equation (2.5.4) can be rewritten as

$$r(t) = x'(t) \cos w_c t - y(t) \sin w_c t \quad (2.5.5)$$

where x' and y are independent Gaussian variates with means

$$\bar{x}' = \sqrt{2S}, \quad \bar{y} = 0 \quad (2.5.6)$$

and variances

$$\overline{(x' - \bar{x}')^2} = \overline{y^2} = N \quad (2.5.7)$$

An error occurs if the phase of $r(t)$ lies outside the correct zone - $\pi/M \leq \theta \leq \pi/M$.

Calculation of P_e :

A simple yet very close approximate result now can be found by calculating the sum of the probabilities

$$P_1 = \text{prob}(y > x' \tan \pi/M) \quad (2.5.8)$$

and

$$P_2 = \text{prob} (y < -x' \tan \pi/M) \quad (2.5.9)$$

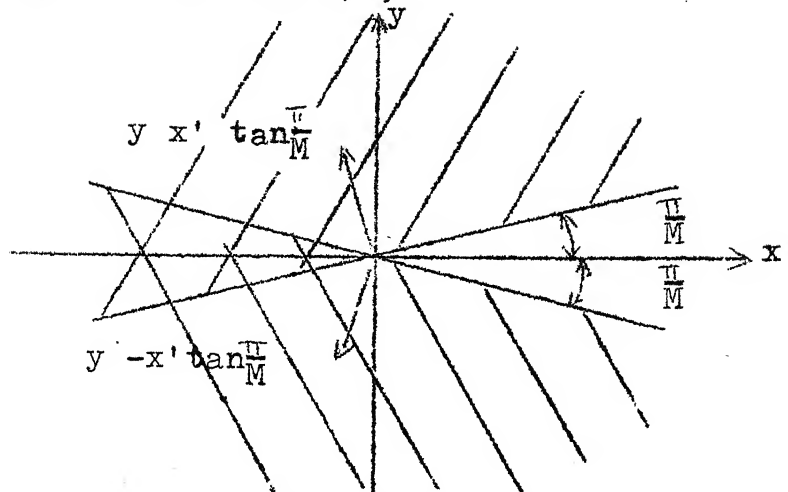


Fig. 2.2: Bounds for errors in M-phase FSK

As shown in Fig. 2.2, $(P_1 + P_2)$ gives the probability that the phasor θ lies outside the zone of correct reception, except that the zone of width $2\pi/M$ has been included twice. It is shown in [1] that at high SNR,

$$(P_1 + P_2) \geq P_e \geq \left(\frac{M-1}{M}\right) (P_1 + P_2) \quad (2.5.10)$$

Therefore for large M

$$P_e \approx P_1 + P_2 \quad (2.5.11)$$

The probabilities P_1 and P_2 have been calculated in [1] as

$$P_1 = P_2 = \frac{1}{2} \text{erfc} (\sqrt{\gamma} \sin \pi/M) \quad (2.5.12)$$

Hence,

$$P_e \approx \text{erfc} (\sqrt{\gamma} \sin \pi/M) \quad (2.5.13)$$

where γ = symbol SNR.

Probability of error in case of 4 phase PSK: [1]

An exact calculation for probability of error in case of 4-phase PSK is possible. If the coordinates of Fig. 2.2 are rotated by 45° and considering 45° phasor to be transmitted, the received quadrature components x' and y are independently Gaussian with variance N and mean as

$$\bar{x}' = \bar{y} = \sqrt{2S} \cos \pi/4 = S \quad (2.5.14)$$

The probability of error is thus given to be

$$P_e = \text{erfc} \sqrt{\gamma/2} (1 - 1/4 \text{erfc} \sqrt{\gamma/2}) \quad (2.5.15)$$

Looking at equation (2.5.13) if we assume fixed information rate operation, it is evident that the SNR per bit ($\gamma_b = \gamma / \log_2 M$) and hence signal power S must be increased as $M^2 / \log_2 M$ if the symbol error probability is maintained constant with increasing M . At the same time required signaling bandwidth diminishes as $1 / \log_2 M$. If we have fixed signaling bandwidth operation, maintaining the same symbol error probability with increasing M requires that SNR per bit γ_b be increased as $M^2 / \log_2 M$ while the information rate increases as $\log_2 M$. Point to be noted, however, is that to compensate for the increased information rate, then transmitted power S must be increased as M^2 and not as $M^2 / \log_2 M$.

Relationship between bit error rates and symbol error rates:[1]

There is no exact relationship between the symbol error rates and bit error rates in most cases. However, it can be approximated in particular cases. In multiphase PSK signaling, as is evident from Fig. 2.1, an error is much more likely to occur with adjacent phases selected than with any of the other phases selected at random. If we select a binary to M-ary coding such that the binary sequences representing adjacent phasors differ in only one bit position (Gray Code) then at high SNRs, the bit error rates and symbol error rates are related as

$$P_{eb} = P_e / \log_2 M \quad (2.5.16)$$

where,

P_{eb} = bit error rate

P_e = symbol error rate

$\gamma_b = \gamma / \log_2 M$ is valid over all SNRs

Calculation of SNR:

For 4-phase PSK, equation (2.5.15) is used for SNR calculations. Equation (2.5.16) gives,

$$P_e = \log_2 M \cdot P_{eb} = 2 P_{eb}$$

Hence for

$$\begin{aligned} P_e &= 2 \times 10^{-4} & ; \quad \gamma_b &= \gamma/2 = 8.4 \text{ db} \\ P_e &= 2 \times 10^{-6} & ; \quad \gamma_b &= \gamma/2 = 10.56 \text{ db} \\ P_e &= 2 \times 10^{-8} & ; \quad \gamma_b &= \gamma/2 = 11.97 \text{ db} \end{aligned}$$

For 8-phase PSK equation (2.5.13) is used for SNR calculations. Equation (2.5.16) gives

$$P_e = \log_2 8 P_{eb} = 3 P_{eb}$$

Hence for

$$\begin{aligned} P_e &= 3 \times 10^{-4} & ; \quad \gamma_b &= \gamma/3 = 11.74 \text{ db} \\ P_e &= 3 \times 10^{-6} & ; \quad \gamma_b &= \gamma/3 = 13.97 \text{ db} \\ P_e &= 3 \times 10^{-8} & ; \quad \gamma_b &= \gamma/3 = 15.44 \text{ db} \end{aligned}$$

Similarly for 16-phase PSK again equation (2.5.13) is used. Equation (2.5.16) gives

$$P_e = 4 P_{eb}$$

Hence for

$$\begin{aligned} P_e &= 4 \times 10^{-4} & ; \quad \gamma_b &= \gamma/4 = 16.15 \text{ db} \\ P_e &= 4 \times 10^{-6} & ; \quad \gamma_b &= \gamma/4 = 18.45 \text{ db} \\ P_e &= 4 \times 10^{-8} & ; \quad \gamma_b &= \gamma/4 = 19.96 \text{ db} \end{aligned}$$

2.5.2 M-ary PSK with differential detection [1]

For large M and at high SNRs, it has been shown in [1] that the approximate probability of error in case of multi-phase

PSK under differential detection is given by

$$P_e = \text{erfc} (\sqrt{2\gamma} \sin \pi/2M) \quad (2.5.17)$$

The above expression gives a very small error for values of $M \geq 4$ and at high SNRs. Since we want the SNRs for BER of 10^{-4} and less, the above result gives accurate enough result for our purpose.

Calculation of SNRs: 4 phase PSK (.DQPSK)

By the help of equation (2.5.16), we can write

$$P_e = \log_2 4 P_{eb} = 2 P_{eb}.$$

Using equation (2.5.17) for SNR calculations one gets,

$$\text{For } P_e = 2 \times 10^{-4} \quad ; \quad \gamma_b = \gamma/2 = 10.7 \text{ db}$$

$$P_e = 2 \times 10^{-6} \quad ; \quad \gamma_b = \gamma/2 = 12.26 \text{ db}$$

$$P_e = 2 \times 10^{-8} \quad ; \quad \gamma_b = \gamma/2 = 14.3 \text{ db}$$

2.6 Minimum Shift Keyed (MSK) and Offset Keyed QPSK Signaling:

Here, we consider the performances of MSK and OK-QPSK and then compare them. The bit error rate calculations are based on the discussions in [7,8,13,16,24] .

It has been seen that if the abrupt phase transitions in the transmitted signal at bit transitions could be avoided, the spectral characteristics of the signal improves considerably. MSK signaling is a particular case of continuous phase FSK

(CP-FSK) signaling where abrupt phase transition is avoided. For the sake of continuity, a brief introduction is given to CP-FSK signaling below. The transmitted signal in case of BFSK is given by

$$s(t) = \begin{cases} A \cos [2\pi f_1 t + \phi(o)] & : '1' \\ A \cos [2\pi f_2 t + \phi(o)] & : '-1' \end{cases} ; 0 \leq t < T \quad (2.6.1)$$

where

$\phi(o)$ = initial phase (assumed constant)

and

f_1, f_2 = two tone frequencies being transmitted.

Let the transmitted CP FSK waveform be written as

$$s'(t) = A \cos [2\pi f_c t + \phi(t)] \quad (2.6.2)$$

where,

$$f_c = (f_1 + f_2)/2 \quad (2.6.3)$$

is the mean of the two tone frequencies ^{of eqn.} \angle (2.6.1). If the two waveforms are to be identical, then $s(t) = s'(t)$ and, we get

$$\begin{aligned} 2\pi f_c t + \phi(t) &= 2\pi f_1 t + \phi(o) & : '1' \\ &= 2\pi f_2 t + \phi(o) & : '-1' \end{aligned} \quad (2.6.4)$$

Using eqn. (2.6.3) in eqn. (2.6.4), we get,

$$\phi(t) = \phi(o) \pm (f_1 - f_2) \pi t \quad (2.6.5)$$

- + sign is for a '1' transmitted
- sign is for a '-1' transmitted

Let $h = T(f_1 - f_2)$ be the modulation index where T is the bit duration, then

$$\phi(t) = \phi(0) \pm \frac{\pi h}{T} t \quad (2.6.6)$$

It has been shown that the value of h is optimum (for minimising the probability of error) at 0.715 [24]. We discuss this case in the next section. The particular case where $h = .5$ is called MSK and is important due to its spectral characteristics. It requires considerably less bandwidth as compared to any of the conventional signaling i.e. PSK, FSK or ASK. MSK is some times called fast frequency shift keying due to the fact that data rate per unit bandwidth is quite high.

The MSK waveform can be represented as below:

$$Y_{\text{MSK}}(t) = \cos(2\pi f_c t + \frac{U_k t}{2T} + x_k) \quad (2.6.7)$$

where,

$U_k = \pm 1$ is bipolar data

$T = \frac{1}{R}$ is bit duration

R = Binary data rate

x_k = a phase constant which is valid over the period

$$kT \leq t \leq (k+1)T$$

As the phase of the waveform is to remain continuous at bit transition interval $t = KT$ and the fact that x_k is constant over $kT \leq t \leq (k+1)T$, we get the recursive formula for x_k as

$$x_k = x_{k-1} + (U_{k-1} - U_k) \frac{\pi k}{2} \quad (2.6.8)$$

For coherent detection a reference value of x_k , say x_0 , can be set to zero without loss of generality. Hence,

$$x_k = 0, \pi \text{ modulo } 2\pi \quad (2.6.9)$$

By using eqns. (2.6.8) and (2.6.9) in eqn. (2.6.7) we can write,

$$\begin{aligned} Y_{MSK}(t) &= \cos x_k \cos 2\pi f_c t \cos \frac{\pi t}{2T} - U_k \cos x_k \sin 2\pi f_c t \sin \frac{\pi t}{2T} \\ &= C(t) \cos 2\pi f_c t \cos x_k - S(t) \sin 2\pi f_c t \cdot U_k \cos x_k \\ &\quad ; \quad KT \leq t \leq (K+1)T \end{aligned} \quad (2.6.10)$$

where

$$C(t) = \cos \frac{\pi t}{2T}$$

$$S(t) = \sin \frac{\pi t}{2T}$$

Here $C(t) \cos x_k \cdot \cos 2\pi f_c t$ can be viewed as 'I' channel and $S(t) U_k \cos x_k \cdot \sin 2\pi f_c t$ as Q channel [7].

Since data U_k can change every T seconds, it might appear that $\cos x_k$ and $U_k \cos x_k$ can also change every T seconds. But on the contrary due to the phase constraint, the two datas can change values at the zero crossings of $C(t)$ for $\cos x_k$ and $S(t)$ for $U_k \cos x_k$. Thus the symbol weighting function in either I or Q channel is a half cycle sinusoidal pulse of duration $2T$ seconds and of alternating sign. The 'I' and 'Q' channels are skewed T seconds to one another. The data is transmitted at a rate of $\frac{1}{2T}$ bits/sec in both I and Q channel. Since $x_k = 0, \pi$ modulo 2π , $\cos x_k$ and $U_k \cos x_k$ can take values only of ± 1 .

From bit to bit independent data U_k , the signs of successive 'I' or 'Q' channel pulses are also random from one $2T$ second pulse to another $2T$ second pulse. Thus when viewed as quadrature signaling waveform we can rewrite eqn. (2.6.10) as

$$Y_{\text{MSK}}(t) = \begin{cases} U_{2k-1} C[t-2kT] \cos 2\pi f_c t - U_{2k-2} S[t-(2k-2)T] \sin 2\pi f_c t & ; (2k-1)T \leq t \leq (2k)T \\ U_{2k-1} C[t-2kT] \cos 2\pi f_c t - U_{2k} S[t-2kT] \sin 2\pi f_c t & ; 2kT \leq t \leq (2k+1)T \end{cases}$$

(2.6.11)

The waveform of OK-QPSK is same as (2.6.11) except for the weighting functions to 'I' and 'Q' channels and is given by [7] as,

$$Y_{\text{OK-QPSK}}(t) = \begin{cases} U_{2k-1} S_{qc}[t-2kT] \cos 2\pi f_c t - U_{2k-2} S_{qs}[t-(2k-2)T] \sin 2\pi f_c t & ; (2k-1)T \leq t \leq 2kT \\ U_{2k-1} S_{qc}[t-2kT] \cos 2\pi f_c t - U_{2k} S_{qs}[t-2kT] \sin 2\pi f_c t & ; 2kT \leq t \leq (2k+1)T \end{cases}$$

(2.6.12)

where

$$S_{qs} = \begin{cases} \frac{1}{\sqrt{2}} & 0 \leq t \leq T \\ 0 & \text{elsewhere} \end{cases}$$

$$S_{qc} = \begin{cases} \frac{1}{\sqrt{2}} & -T \leq t \leq T \\ 0 & \text{elsewhere} \end{cases}$$

The encoding used in (2.6.11) is to demultiplex the data streams which are used to determine the symbol pulse signs of 'I' and 'Q' channels during odd intervals $(2k-1)T \leq t \leq (2k+1)T$ and even intervals $2kT \leq t \leq (2k+2)T$ respectively.

In case of MSK when the bandwidth is infinite there is no ISI between 'I' and 'Q' channels.

In offset QPSK signaling, the bit transitions for one binary channel occur at the middle of the bit interval for the other channel. Under the assumption of independent equally-likely choices of positive or negative polarities for each bit, the probability of transition is one half when a transition occurs, the cross-coupling between 'I' and 'Q' channels changes polarity at mid bit of the other binary channel and the inter channel interference during the first half of the bit interval is consequently cancelled by the interference of opposite polarity during the second half of the interval. Hence, detection performance of OK-QPSK is identical to BPSK when a bit transition occurs. If no transition occurs, then the cross-coupling interference remains constant during the entire interval of the detected bit. Hence the performance of OK-QPSK is between BPSK and QPSK under any conditions.

If the binary data rate is same for MSK, QPSK and OK-QPSK (i.e. $\frac{1}{T}$) then the phase transitions in MSK and offset QPSK waveforms occur every T seconds whereas the conventional QPSK has the transitions occurring every 2T seconds. QPSK and OK-QPSK have abrupt phase transitions. In OK-QPSK, the transitions can be only $\pm 90^\circ$ whereas in

QPSK, 180° phase reversals are possible. Therefore OK-QPSK performs better than QPSK. The continuous phase nature of MSK gives it superior spectral characteristics than either QPSK or OK-QPSK. The bandwidth occupied by OK-QPSK (or QPSK) is one half of that of BPSK for same data rate transmission although penalty is paid for thisⁱⁿ QPSK (or OK-QPSK) in terms of increased signal power.

MSK can be non-coherently detected using a discriminator. This provides an inexpensive method of demodulation. The degree of regeneration of filter side lobes is less in case of both MSK or OK-QPSK than conventional QPSK if they are band limited. Either technique has a carrier recovery feature which provides an advantage over conventional QPSK. The drawback is that both the techniques require a certain critical bandwidth and, for narrower channels, performance degrades due to ISI. MSK is found to be superior to that of QPSK when the channel bandwidth exceeds 1.1 times the binary data rate [7].

For BER calculations we assume the channel to be ideal (defined as linear, infinite bandwidth channel, corrupted by additive white gaussian noise only). In addition, perfect carrier and timing references are assumed available at the receiver. With these assumptions, and viewing both MSK and

OK-QPSK as orthogonal binary channels with antipodal signaling, the binary error probability is given by [3] as

$$P_e = \frac{1}{2} \operatorname{erfc}(\sqrt{\gamma}) \quad (2.6.13)$$

where $\gamma = E_b/N_0$

= SNR per bit

E_b = Energy per bit

$N_0/2$ = double sided spectral density of WGN.

The SNR calculations are same as BPSK case.

2.7.1 Continuous Phase FSK(CPFSK $h = .715$): coherent detection [6,12]

In previous section, an introduction to CPFSK was given. In this section we shall deal with the probability of error calculations when $h = 0.715$. Instead of observing a single bit and making decision on that bit we shall be making decision on a bit by observing 'n' bits i.e. decision on first bit is made on the basis of observed waveform during that bit interval and (n-1) subsequent bit intervals. We assume that the information bits are ± 1 and the only interference present is the additive white Gaussian noise with double sided spectral density as $N_0/2$.

The CPFSK waveform can be represented during the first bit interval as:

$$s(t) = \cos(w_c t + \frac{a_1 \pi h t}{T} + \theta_1); 0 \leq t \leq T \quad (2.7.1)$$

where a_1 = binary data

$$= \pm 1$$

h = modulation index defined as the peak-to-peak frequency deviation divided by the bit rate $(\frac{1}{T})$.

w_c = angular carrier frequency

θ_1 = R.F. phase at the beginning of the observation interval.

With the constraint that the phase of $s(t)$ is to remain continuous, the waveform during the 'i'th bit interval can be written as

$$s(t) = \cos \left[w_c t + \frac{a_i \pi h (t - (i-1)T)}{T} + \sum_{j=1}^{i-1} a_j \pi h + \theta_1 \right] \quad ; (i-1)T \leq t \leq iT \quad (2.7.2)$$

Since we are dealing with coherent detection case, θ_1 can be assumed to be zero without loss of generality. Equation (2.7.2) can now be put in the following form:

$$s(t, a_1, A_k) = \cos \left[w_c t + \frac{a_i \pi h (t - (i-1)T)}{T} + \sum_{j=1}^{i-1} a_j \pi h \right] \quad ; (i-1)T \leq t \leq iT \quad (2.7.3)$$

where a_1 = binary data on which a decision is to be made and A_k represents a particular data sequence i.e. it represents a $(n-1)$ tuple a_2, a_3, \dots, a_n .

Our aim is now to observe $s(t, a_1, A_k)$ in AWGN and produce an optimum decision as to the polarity of a_1 . The problem thus presented is a composite hypothesis problem which has been treated in [4]. The solution is well known. The likelihood ratio, l , can be expressed as

$$l = \frac{\int_A \exp\left(\frac{2}{N_0} \int_0^{nT} r(t) s(t, 1, A) dt\right) f(A) dA}{\int_A \exp\left(\frac{2}{N_0} \int_0^{nT} r(t) s(t, -1, A) dt\right) f(A) dA} \quad (2.7.4)$$

where

$$\int_A dA = \int_{a_2} \int_{a_3} \dots \int_{a_n} da_2 da_3 \dots da_n \quad (2.7.5)$$

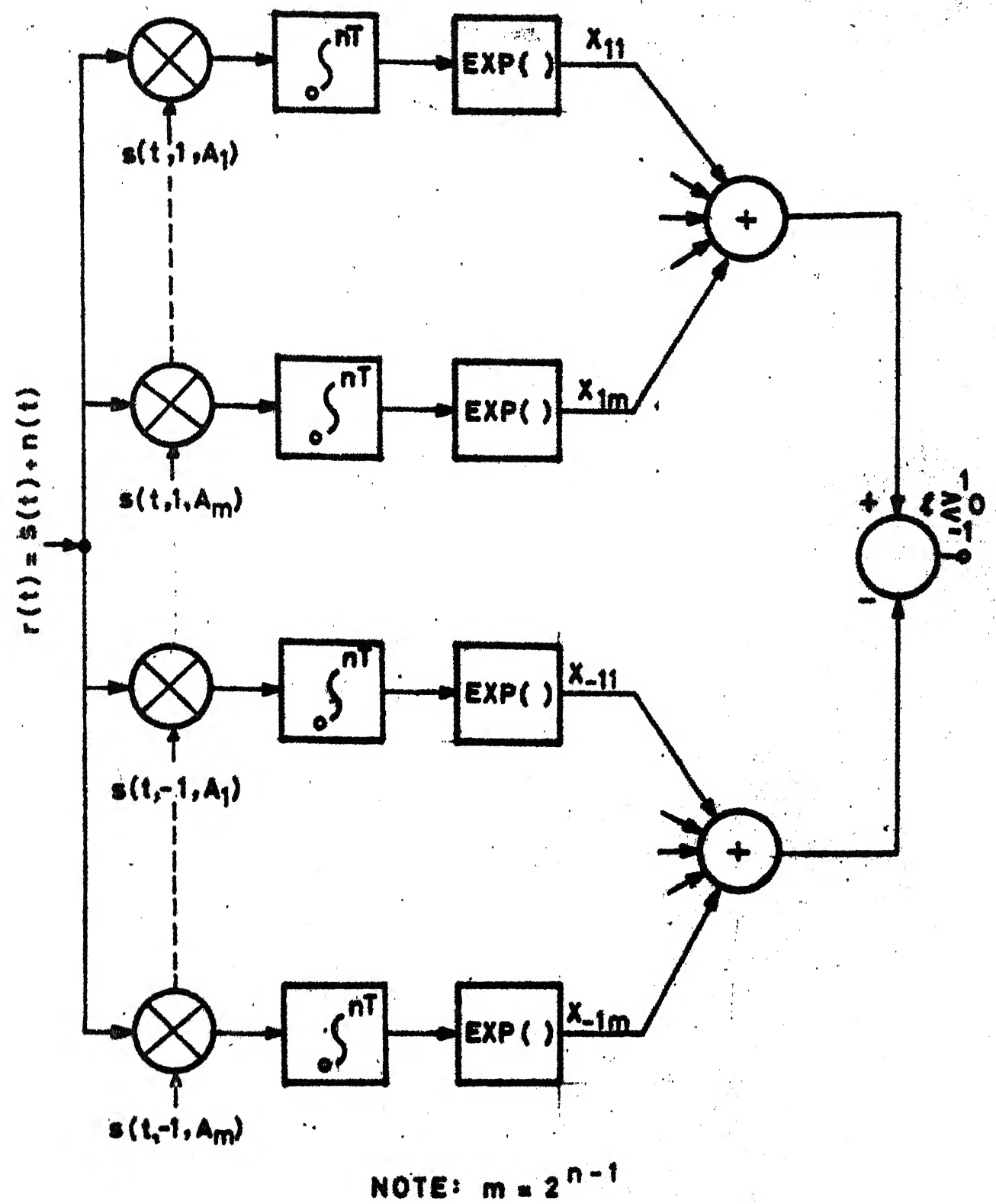
Since a_i 's are assumed independent, the density of A is given by

$$f(A) = f(a_2) f(a_3) \dots f(a_n) \quad (2.7.6)$$

where $f(a_i)$ is the density function of i th data bit.

$$f(a_i) = \frac{1}{2} \delta(a_i - 1) + \frac{1}{2} \delta(a_i + 1) \quad (2.7.7)$$

Using equation (2.7.7) in equation (2.7.4) and carrying out the integration, likelihood ratio ' l ' is given as [6,12]



2.3 Block diagram of optimum CPFSK coherent receiver

$$l = \frac{\exp\left(\frac{2}{N_0} \int_0^{nT} r(t)s(t,1,A_1)dt\right) + \dots + \exp\left(\frac{2}{N_0} \int_0^{nT} r(t)s(t,1,A_m)dt\right)}{\exp\left(\frac{2}{N_0} \int_0^{nT} r(t)s(t,-1,A_1)dt\right) + \dots + \exp\left(\frac{2}{N_0} \int_0^{nT} r(t)s(t,-1,A_m)dt\right)} \quad (2.7.8)$$

where

$$m = 2^{n-1}$$

The receiver structure defined by equation (2.7.8) is shown in Figure 2.3.

It is not possible to find an exact expression in closed form for probability of error for the receiver shown in Figure 2.3. But it is possible to find a bound on the performance of the receiver, both at high and low SNRs (upper as well as lower bounds). Since our interest is in BERs of 10^{-4} and less and hence high SNR, we shall find the bound applicable at high SNRs only. Applying the union bound to our case which is tight at high SNRs [12], we get

$$P_e \leq \frac{1}{m} \sum_{l=1}^m \sum_{j=1}^m \Pr \{x_{1l} \leq x_{-1j} / s(t,1,A_l)\} \quad (2.7.9)$$

where x_{1l} is the output of correlator matched to signal $s(t,1,A_l)$ and x_{-1j} to $s(t,-1,A_j)$. Further,

$$\begin{aligned} \Pr [x_{11} \leq x_{-1j} | s(t, 1, A1)] \\ = \frac{1}{2} \operatorname{erfc} \left[\left\{ \frac{nEb}{N_0} (1 - \rho(1, j)) \right\}^{1/2} \right] \end{aligned} \quad (2.7.10)$$

where E_b = energy per bit

and

$$\rho(1, j) = \frac{1}{nE_b} \int_0^{nT} s(t, -1, A1) s(t, 1, A_j) dt \quad (2.7.11)$$

$\rho(1, j)$ is correlation coefficient. Equation (2.7.11) is calculated using equation (2.7.3) and is given as 6

$$\rho(1, j) = \frac{1}{n} \sum_{k=1}^n \operatorname{sinc} (h/2(a_k - b_k)) \cdot \cos \left[\frac{\pi h}{2} (a_k - b_k) + \sum_{j=1}^{k-1} \pi h (a_j - b_j) \right] \quad (2.7.12)$$

where a_i 's are data bits belonging to sequence A1 and b_i 's are data bits belonging to sequence A_j with the constraint $a_1 = 1$ and $b_1 = -1$.

Lower bound on performance:

A lower bound on the performance can be evaluated by supposing that for each transmitted sequence, the receiver needs only to decide between that sequence and its nearest neighbour. This receiver will perform as well as the receiver which does not know which of the two sequences were

transmitted but must compare with all possible sequences. This performance is a lower bound to that presented earlier in equation (2.7.9).

$$P_e \geq \frac{1}{m} \sum_{l=1}^m \frac{1}{2} \operatorname{erfc} \left[\left\{ \frac{nE_b}{N_0} (1 - \rho^*(l)) \right\}^{1/2} \right] \quad (2.7.13)$$

where $\rho^*(l) = \text{maximum of } \rho(l, j) \text{ over all } j$.

Discussion of Numerical results:

Numerical evaluations have been made for upper bound and lower bounds at high SNRs for 2 bits, 3 bits, and 5 bits observations intervals. The graph is shown in Figure 2.4.

Conclusions:

It is seen that at high SNRs, the upper and lower bound curves merge together. There is apparently hardly any difference between the two above 8 dB SNR. It is observed that there is a significant gain in terms of SNR when the observation interval is increased from 2 to 3 bits. But when the interval is increased from 3 to 5 bit, the gain in terms of SNR is not that pronounced. Therefore it can be concluded that 3 bits observation interval at high SNR is sufficient as increasing the observation interval to 5 bits improves the performance of the receiver only very marginally.

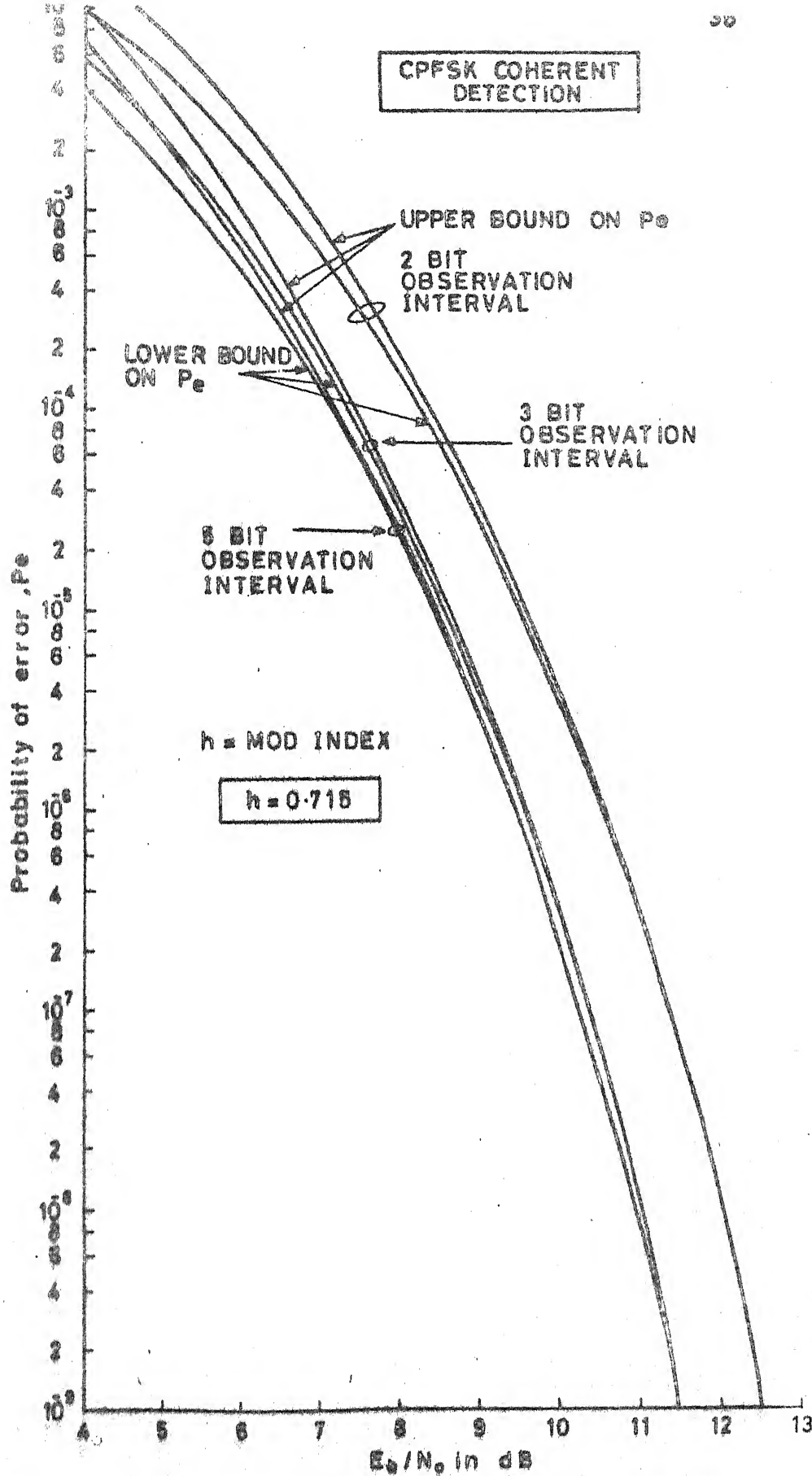


Fig 2.4 Performance of coherent CPFSK receiver

Table 2.1
Lower Bound on Probability of Error

SNR (Eb/No) dB	Observation interval = 2 Bit	Observation interval = 3 Bit	Observation interval = 5 Bit
1	5.035×10^{-2}	3.626×10^{-2}	2.816×10^{-2}
2	3.293×10^{-2}	2.199×10^{-2}	1.650×10^{-2}
3	1.967×10^{-2}	1.194×10^{-2}	8.671×10^{-3}
4	1.052×10^{-2}	5.653×10^{-3}	3.987×10^{-3}
5	4.905×10^{-3}	2.254×10^{-3}	1.559×10^{-3}
6	1.932×10^{-3}	7.264×10^{-4}	4.990×10^{-4}
7	6.188×10^{-4}	1.793×10^{-4}	1.244×10^{-4}
8	1.534×10^{-4}	3.175×10^{-5}	2.264×10^{-5}
9	2.770×10^{-5}	3.714×10^{-6}	2.758×10^{-6}
10	3.369×10^{-6}	2.586×10^{-7}	2.018×10^{-7}
11	2.492×10^{-7}	9.413×10^{-9}	7.736×10^{-9}
12	9.837×10^{-9}	1.516×10^{-10}	1.311×10^{-10}
13	1.750×10^{-10}	8.807×10^{-13}	7.951×10^{-13}
14	1.136×10^{-12}	1.411×10^{-15}	1.321×10^{-15}
15	2.066×10^{-15}	4.477×10^{-19}	4.307×10^{-19}

Table 2.2

Upper Bound on Probability of Error

SNR (Eb/No) dB	Observation interval = 2 Bit	Observation interval = 3 Bit	Observation interval = 5 Bit
1	9.037×10^{-2}	8.727×10^{-2}	1.0533×10^{-1}
2	5.769×10^{-2}	4.816×10^{-2}	4.809×10^{-2}
3	3.344×10^{-2}	2.349×10^{-2}	1.945×10^{-2}
4	1.722×10^{-2}	9.881×10^{-3}	6.960×10^{-3}
5	7.670×10^{-3}	3.482×10^{-3}	2.196×10^{-3}
6	2.858×10^{-3}	9.941×10^{-4}	6.008×10^{-4}
7	8.578×10^{-4}	2.203×10^{-4}	1.358×10^{-4}
8	1.979×10^{-4}	3.584×10^{-5}	2.345×10^{-5}
9	3.319×10^{-5}	3.955×10^{-6}	2.791×10^{-6}
10	3.773×10^{-6}	2.661×10^{-7}	2.024×10^{-7}
11	2.647×10^{-7}	9.516×10^{-9}	7.741×10^{-9}
12	1.010×10^{-8}	1.523×10^{-10}	1.311×10^{-10}
13	1.766×10^{-10}	8.815×10^{-13}	7.951×10^{-13}
14	1.139×10^{-12}	1.411×10^{-15}	1.321×10^{-15}
15	2.067×10^{-15}	4.477×10^{-19}	4.307×10^{-19}

In cases where the performance must be improved beyond the results so obtained, there is no other alternative but to use error correcting codes.

Coherent CPFSK out performs BPSK coherent detection scheme with a modulation index (h) of 0.715 and observation interval of 3 bit or more. The gain in SNR is 1 db at a BER of 10^{-4} as compared to BPSK case. Inspite of the better theoretical performance of this scheme, practical difficulties make it a difficult system for realization. This is due to the fact that there is no simple technique for obtaining the reference signal required for coherent detection of CPFSK from the received waveform for a modulation index of 0.715 (which produces the best performance).

SNRs needed for various probabilities of errors are shown in Table 2.4.

2.7.2 CPFSK($h = 0.715$): Non-coherent detection: [6,12]

In this section we shall discuss a receiver structure and find an upper bound on probability of error when the carrier phase is unknown. We shall be making decision on the present bit by n past bits and n bits which would arrive later on i.e. the decision on a bit is based on observation of $(2n+1)$ bits. The signal component in the received waveform

corresponding to the transmitted CPFSK waveform can be written as (refer equation 2.7.2)

$$s(t) = (2P)^{1/2} \cos \left[\left(\omega_c t + \frac{a_i \pi h(t - (i-1)T)}{T} + \sum_{j=1}^{i-1} a_j \pi h + \theta_1 \right) \right]$$

$$; 0 \leq t \leq T$$

(2.7.14)

We can denote the observed waveform as $s(t, a_{n+1}, A_k, \theta_1)$ where A_k denotes the $2n$ tuples $a_1, a_2, \dots, a_n, a_{n+2}, \dots, a_{2n+1}$. a_1 's are assumed to be equally probable to be ± 1 and are independent. The phase θ_1 is assumed to be uniformly distributed between $\pm \pi$. We want to design a receiver which observes $(2n+1)$ bits of information and makes a decision regarding the polarity of a_{n+1} with the objective to minimise decision error. Following the argument of previous section, the likelihood ratio for this composite hypothesis can be expressed as

$$l = \frac{\int_{\theta_1} \int_A f(A) f(\theta_1) \exp\left(\frac{2}{N_0} \int r(t) s(t, 1, A, \theta_1) dt\right) d\theta_1 dA}{\int_{\theta_1} \int_A f(A) f(\theta_1) \exp\left(\frac{2}{N_0} \int r(t) s(t, -1, A, \theta_1) dt\right) d\theta_1 dA}$$

(2.7.15)

The only difference between this likelihood ratio and that obtained in the previous section given by Eqn. (2.7.4)

is that one should suitably account for the uncertainty because of random phase. The decision is made here on the middle bit rather than first bit. One could write analogous to equation (2.7.8)

$$l = \frac{\int_{\theta_1} \sum_{k=1}^{m'} \left(\frac{2}{N_0} \int r(t) s(t, 1, A_k, \theta_1) dt \right) f(\theta_1) d\theta_1}{\int_{\theta_1} \sum_{k=1}^{m'} \left(\frac{2}{N_0} \int r(t) s(t, -1, A_k, \theta_1) dt \right) f(\theta_1) d\theta_1} \quad (2.7.16)$$

where $m' = 2^{2n}$

Averaging over the random phase of Equation (2.7.16) gives a result introducing modified Bessel function of zero order. We can write the above equation as [12]

$$l = \frac{\sum_{i=1}^{m'} I_0\left(\frac{2}{N_0} Z_{1i}\right)}{\sum_{i=1}^{m'} I_0\left(\frac{2}{N_0} Z_{-1i}\right)} \quad (2.7.17)$$

where

$$Z_{1i}^2 = \left(\int r(t) s(t, 1, A_i, 0) dt \right)^2 + \left(\int r(t) s(t, 1, A_i, \pi/2) dt \right)^2$$

and

$$Z_{-1i}^2 = \left(\int r(t) s(t, -1, A_i, 0) dt \right)^2 + \left(\int r(t) s(t, -1, A_i, \pi/2) dt \right)^2$$

The receiver structure given by equation (2.7.17) is shown in Figure 2.5.

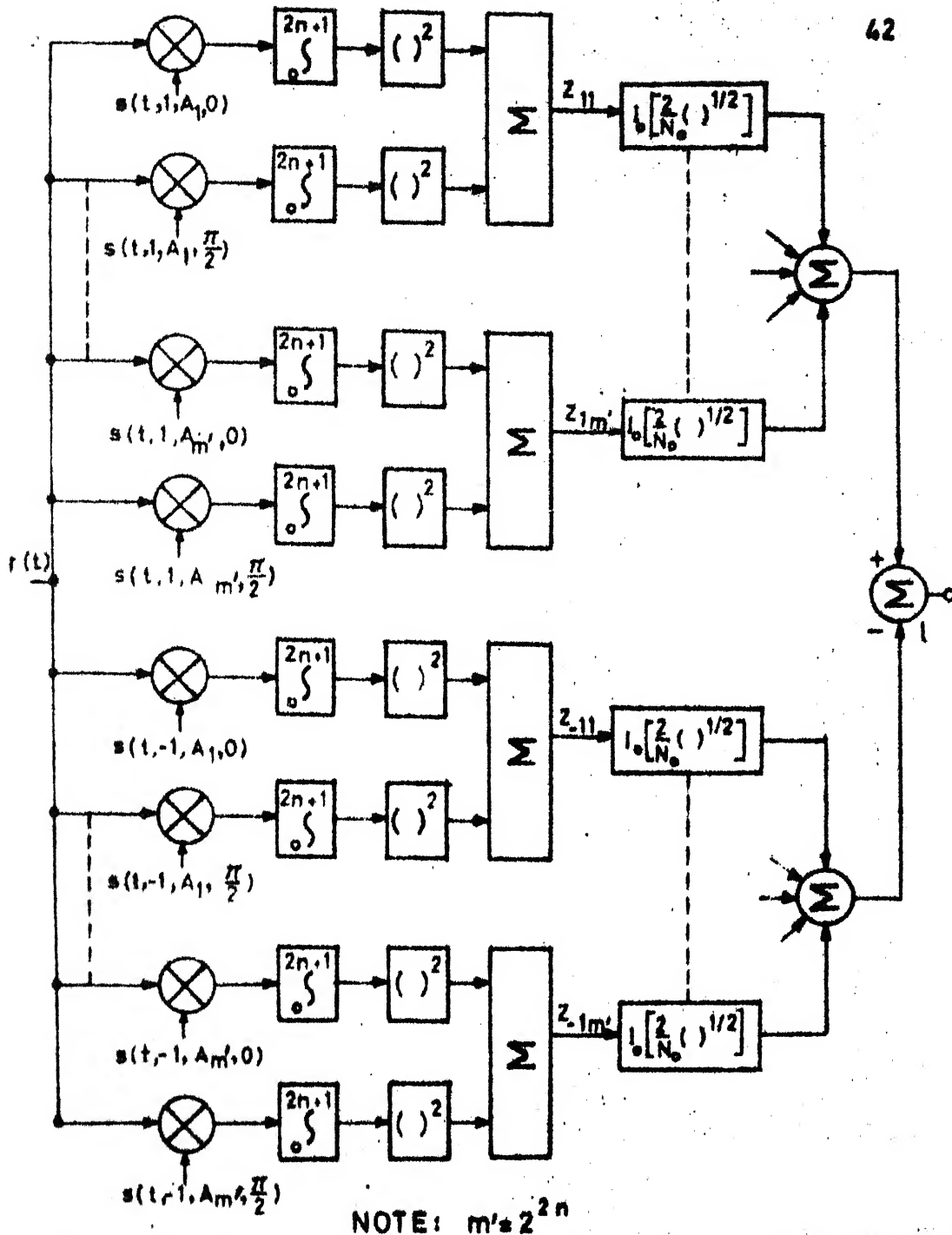


Fig. 2.5 Block diagram of optimum CPFSK non-coherent receiver.

It is not possible to analytically derive an expression for probability of error in a closed form for the receiver shown in Figure 2.5. However it is possible to find an upper bound on the performance which is tight on high SNRs.

High SNR bound on P_e :

It is known that for large argument

$$\sum_i I_0(x_i) \approx I_0(x_1) \quad (2.7.18)$$

where x_1 is the largest of the set x_i . Using this approximation, the equation (2.7.17) can be written as

$$I_0\left(\frac{2}{N_0} Z_{11}\right) \approx \sum_{-1}^1 I_0\left(\frac{2}{N_0} Z_{-1k}\right) \quad (2.7.19)$$

where Z_{11} is largest of the set $\{Z_{1i}\}$ and Z_{-1k} is largest of the set $\{Z_{-1i}\}$. As $I_0(\cdot)$ is monotonic function of its argument, the equation (2.7.19) is equivalent to

$$Z_{11} \approx \sum_{-1}^{+1} Z_{-1k} \quad (2.7.20)$$

The demodulator using the strategy of equation (2.7.20) would choose the largest of all Z_{ki} and then classify the largest as corresponding to a data '1' or data '-1' in the middle bit interval. A decision error is made if, given a '1' was transmitted one of the Z_{-1i} was largest.

Suppose that a $(2n+1)$ bits transmitted word is observed and the middle bit is a data 1. The transmitted sequence, excluding the middle bit, is indicated by the index 'k' so that an error is made if at least one of $\{Z_{-1j}\}$ is greater than Z_{1k} . Then by the union bound [3]

$\Pr (\text{Error/sequence } k \text{ transmitted})$

$$\leq \sum_{j=1}^{m'} \Pr (Z_{-1j} > Z_{1k}) \quad (2.7.21)$$

The average probability of error can now be computed by averaging over all possible transmitted sequences containing a 1 in the middle bit interval.

$$P_e = \frac{1}{m'} \sum_{k=1}^{m'} \Pr (\text{Error/sequence } k \text{ transmitted})$$

$$P_e \leq \frac{1}{m'} \sum_{k=1}^{m'} \sum_{j=1}^{m'} \Pr (Z_{-1j} > Z_{1k}) \quad (2.7.22)$$

In equation (2.7.22) the bounding performance of equation (2.7.20) has been reduced to a simple binary problem; solution of which is well known [5]. For this situation

$$\Pr (Z_{-1j} > Z_{1k}) = \frac{1}{2} \left[1 - Q(b^{1/2}, a^{1/2}) + Q(a^{1/2}, b^{1/2}) \right] \quad (2.7.23)$$

where $Q(',')$ is Marcum's function defined by equation (2.2.6) and 'a' and 'b' are given by

$$\begin{Bmatrix} b \\ a \end{Bmatrix} = (2n+1) \frac{E_b}{2N_0} \left[1 \pm (1 - |\rho|^2)^{1/2} \right] \quad (2.7.24)$$

where

+ is used for 'b'

- is used for 'a'.

$\frac{E_b}{2N_0}$ is the SNR of Z_{1k} . Whereas $(2n+1) \frac{E_b}{N_0}$ is the SNR for $(2n+1)$ bits

$\rho =$ is the value of correlation between the transmitted waveforms corresponding to sequence j, with a data -1 in the middle bit interval, and sequence k, with a data 1 in the middle bit interval. It is given by [12] as

$$\begin{aligned} &= \frac{1}{2n+1} \sum_{k=1}^{2n+1} \exp \left(j \sum_{i=1}^{k-1} (a_i - b_i) \pi h \right) \\ &\quad \cdot \exp \left(\frac{j\pi h}{2} (a_k - b_k) \right) \cdot \text{sinc} \left(h/2(a_k - b_k) \right) \end{aligned} \quad (2.7.25)$$

where b_k belongs to kth bit sequence of data $\{b_k\}$ and a_k to jth bit sequence of data with the constraint that $b_{n+1} = 1$ and $a_{n+1} = -1$.

Table 2.3

Probability of Errors for BPSK and CPFSK non-coherent
detector

SNR= $\frac{E_b}{N_0}$ dB	BPSK P_e	Upper Bound	
		Observation interval = 3 bit P_e	Observation interval = 5 bit P_e
1	5.628×10^{-2}	-	-
2	3.750×10^{-2}	-	-
3	2.287×10^{-2}	1.393×10^{-1}	$1.196 \cdot 10^{-1}$
4	1.250×10^{-2}	7.363×10^{-2}	4.675×10^{-2}
5	5.953×10^{-3}	3.375×10^{-2}	1.528×10^{-2}
6	2.388×10^{-3}	1.303×10^{-2}	4.065×10^{-3}
7	7.726×10^{-4}	4.084×10^{-3}	8.485×10^{-4}
8	1.909×10^{-4}	9.917×10^{-4}	1.319×10^{-4}
9	3.362×10^{-5}	1.758×10^{-4}	1.420×10^{-5}
10	3.872×10^{-6}	2.115×10^{-5}	9.862×10^{-7}
10.2	-	-	5.839×10^{-7}
10.5	-	-	2.933×10^{-7}
11	2.613×10^{-7}	1.575×10^{-6}	-
11.2	1.412×10^{-7}	8.270×10^{-7}	-
11.5	-	3.203×10^{-7}	-
11.7	-	1.303×10^{-7}	-

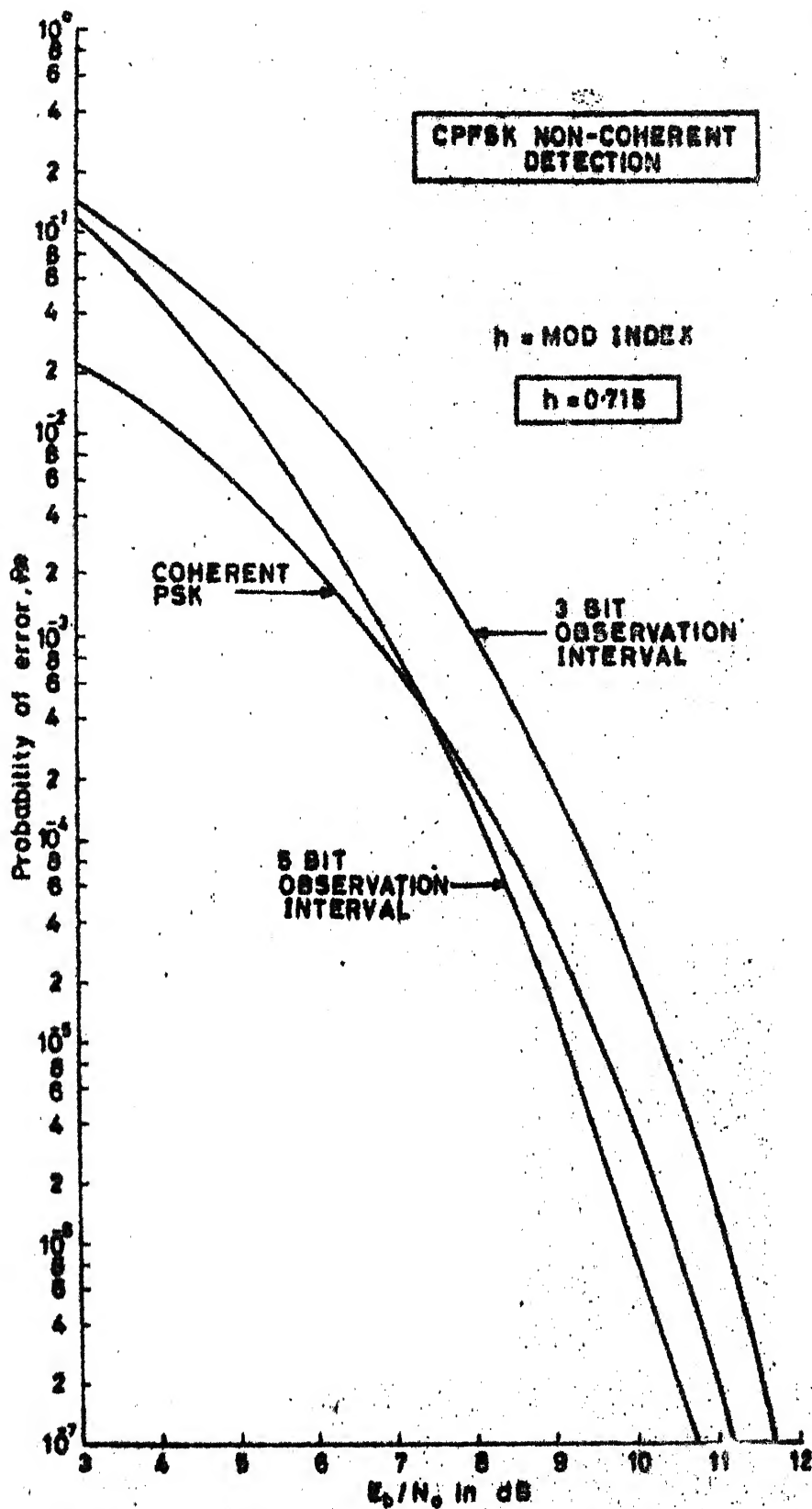


Fig. 2-6. Performance of non-coherent CPFSK receiver

Discussion of numerical results:

Numerical calculations have been made for upper bound on P_e for 3 bits and 5 bits observation intervals for high SNR. To compare the performance of this non-coherent receiver with BPSK case, calculations have been made for BPSK case also. A graph has been plotted in Figure 2.6 where SNR versus P_e is shown.

Marcum Q function has been computed using the algorithm of reference [21]. This gives an accuracy upto 10^{-8} . The programme is given in Appendix A.

Conclusions:

Non-coherent CPFSK receiver has been compared with BPSK receiver with one bit observation interval for which it gives best performance. Looking at the Figure 2.6, it is seen that at SNR lower than 8 dB (approx.) BPSK (coherent detection) performance is better than CPFSK performance both with 3 bits and 5 bits observation intervals. But at SNR > 8 dB, 5 bits non-coherent CPFSK receiver out performs BPSK scheme. At lower SNRs, the advantage gained by increasing the observation interval from 3 bits to 5 bits is not very significant. But at higher SNRs, there is a significant improvement. For a BER of 10^{-6} , the gain is approximately 1.3 dB but at BER of 10^{-2} gain is only of the order of 0.6 dB.

A comparative study of Figures 2.4 and 2.6 show that at $\text{BER} \leq 10^{-5}$, the non-coherent and coherent receiver with 5 bits observation intervals are equivalent in performance to within 0.5 dB. This shows that extending the observation interval beyond 5 bits is not going to improve the performance of non-coherent receiver by more than 0.5 dB approximately.

The fact that 5 bits CPFSK non-coherent detector performs better than coherent BPSK and has a better power spectral distribution than BPSK in terms of percentage power contained in a given bandwidth, makes CPFSK non-coherent detection an attractive scheme for channels whose performance is limited by thermal noise. This scheme also does not have the synchronisation problem as is the case with coherent structure and is realizable using available technology. The cost is to be paid in terms of additional complexity of the receiver. SNRs needed for various probabilities of errors are shown in Table 2.4.

2.8 Comparison of the modulation schemes under ideal conditions:

Discussion:

Table 2.4 has been prepared to portray the significant differences in SNR needed ^{for} various BERs using

Table 2.4

Ideal performance of representative modulation schemes

Modulation schemes	SNR = Eb/No (dB)		
	Pe=10 ⁻⁴	Pe=10 ⁻⁶	Pe=10 ⁻⁸
OOK: Coherent detection	11.4	13.56	14.9
OOK: Envelope detection	11.9	14.2	15.5
PSK: Coherent detection	11.4	13.56	14.9
FSK: Non-coherent detection	12.5	14.1	15.5
BPSK:	8.4	10.54	11.97
DPSK:	9.3	11.18	12.49
QPSK:	8.4	10.54	11.97
8-PSK:	11.74	13.97	15.44
16-PSK:	16.15	18.45	19.96
DQPSK:	10.7	12.86	14.3
OK-QPSK	8.4*	10.54	11.97
MSK(h= .5)	8.4*	10.54	11.97
CPFSK: Coherent detection h = .715	7.4 [#]	9.55	10.98
CPFSK: Non-coherent detection h= .715	9.3	11.15	-

*Under ideal conditions, BER performances of OK-QPSK and BPSK are same. Also BER performance of MSK is same as BPSK under ideal conditions and under the assumptions of Section 2.6.

[#]Assumes an observation interval of 3 bits.

different modulation techniques under white Gaussian noise assumptions. Symbolic BERs of 10^{-4} (Voice grade Communication), 10^{-6} (video) and 10^{-8} (high accuracy data) have been selected for the calculation of SNRs. The values obtained are for ideal conditions. The SNRs in case of OOK (coherent and non-coherent schemes) has been shown to be 3 dB lesser than shown in many other texts. This is due to the fact that average SNR has been considered throughout. The symbol error rates have been converted ^{to} bit error rates and symbol SNRs have been converted to bit SNRs. The most interesting result is that coherent CFFSK ($h = .715$) outperforms BPSK and other equivalent techniques (which are optimum only when the observation interval is confined to one bit). The identical performances of MSK, QPSK and OK-QPSK attests to their underlying similarities. Indeed these techniques differ only in the weighting functions applied to 'I' and 'Q' channels.

Any practical system will deviate from the results obtained in Table 2.4 and should be suitably accounted for. We discuss some of the departures in subsequent chapters.

CHAPTER 3

COMMUNICATION EFFICIENCY

3.1 INTRODUCTION:

In this chapter, efficiencies of certain digital modulation techniques, as measured by data rate per unit bandwidth, have been compared. The systems compared are FSK, PSK and linear modulation systems. In each case the channel is assumed to be AWGN, linear and without any ISI. Our aim is to find the maximum achievable data rate per unit bandwidth for a given SNR and probability of error. The calculations have been made assuming optimum detection (optimum detector achieves the smallest possible error rate for fixed input SNR).

3.2 Frequency-Shift-Keying:

FSK system under discussion generates one of 'M' possible tones of fixed duration T and unit energy. The 'l'th tone can be represented by

$$S_l(t) = \left(\frac{2}{T}\right)^{1/2} \cos (\omega_c t + l \Delta \omega t) ,$$
$$0 \leq t \leq T; l = 1, 2, \dots, M \quad (3.2.1)$$

where

ω_c is angular carrier frequency and $\Delta \omega$ is the minimum angular frequency deviation.

The optimum detector for this set of signals operating over the additive white Gaussian channel of double sided spectral density of N_0 watt/Hz is treated in [3]. It consists of a bank of 'M' matched filters; the filters are matched to the signal set $\{S_l(t)\}$. An equivalent technique employs a bank of 'M' correlators (integrate-and-dump circuits) giving rise to 'M' quantities,

$$x_l = \int_0^T S_l(t) v(t) dt \quad (3.2.2)$$

$$l = 1, 2 \dots M$$

where $v(t)$ is the received waveform.

The optimum detector makes decision based on the set of random variables $\{x_l\}$. It decides $S_j(t)$ was transmitted when

$$x_j = \max x_l \quad (3.2.3)$$

One can derive an expression for probability of error but it is sufficient and also mathematically tractable to use the tight upper bound on the probability of error by using the Union-Bound which states that the probability of union of 'M' events is always smaller than or equal to the sum of the probabilities of 'M' individual events [3]. There is no significant difference in the performance of FSK

coherent optimum detector and non-coherent optimum detector at high SNRs [2]. Since our interest lies in the probability of errors of 10^{-4} and smaller and as such high SNRs, the upper bound can be written as

$$P_e \leq (M-1) e^{-\frac{E}{2N_0} (1-\rho)} \quad (3.2.4)$$

where E is the signal energy and ρ is the maximum cross-correlation coefficient between the signal set $\{S_i(t)\}$. It is given by

$$\begin{aligned} &= \max_{i,j; i \neq j} \rho_{ij} = \max_{i,j; i \neq j} \int_0^T S_i(t) S_j(t) dt \\ & \quad (3.2.5) \end{aligned}$$

Substituting the values of $S_i(t)$ and $S_j(t)$ into equation (3.2.5) and solving, we get

$$\begin{aligned} &= \max_{i,j; i \neq j} \frac{\sin(i-j) \Delta \omega T}{(i-j) \Delta \omega T} = \frac{\sin \Delta \omega T}{\Delta \omega T} \\ & \quad (3.2.6) \end{aligned}$$

Our interest lies in $P_e \leq 10^{-4}$ and consequently large exponents of equation (3.2.4). Therefore we can replace the inequality in equation (3.2.4) by equality. Furthermore, at large SNRs, the contribution due to the factor $(M-1)$ is minor and we can neglect it. Hence,

$$P_e = e^{-\frac{E}{2N_0} (1-\rho)} \quad (3.2.7)$$

Our aim is to maximise the data rate per unit bandwidth associated with the signal set $\{S_1(t)\}$, keeping the probability of error and SNR constant. The data rate 'R' can be expressed as

$$R = N \log_2 M = N 1.443 \ln M \quad (3.2.8)$$

where

$$N = \frac{1}{T} \text{ is the signaling rate.}$$

A reasonable measure of bandwidth 'B' in case of FSK can be expressed as [22]

$$B = N + (M-1) \Delta f \quad (3.2.9)$$

where

$$\Delta f = \Delta \omega / 2\pi$$

Thus,

$$\frac{R}{B} = \frac{1.443 \ln M}{1 + (M-1) \frac{\Delta f}{N}} \quad (3.2.10)$$

The argument of the exponent in equation (3.2.7) can now be written as

$$\begin{aligned} \frac{E}{2N_0} (1-\rho) &= \frac{E}{2N_0} \frac{B}{N} \frac{N}{N} [1-g(y)] \\ &= \gamma \left(\frac{B}{N} \right) [1-g(y)] \end{aligned} \quad (3.2.11)$$

where γ is average SNR in a bandwidth of B Hz and

$$g(y) = \frac{\sin \frac{2\pi \Delta f/N}{2\pi \Delta f/N}}{2\pi \Delta f/N} = \frac{\sin 2\pi y}{2\pi y} \quad (3.2.12)$$

where

$$y = \frac{\Delta f}{N}$$

Thus equation (3.2.7.) can be rewritten as

$$P_e = e^{-\gamma \frac{B}{N} [1-g(y)]} \quad (3.2.13)$$

With the help of equations (3.2.9) and (3.2.13) we can write

$$\frac{B}{N} = 1+(M-1)y = \frac{1}{\gamma} \ln \frac{1}{P_e} [1-g(y)]^{-1} \quad (3.2.14)$$

For a given P_e and γ , M and y are related by the above expression. Using the value of 'M' in terms of y and $g(y)$ from equations (3.2.14) into (3.2.10) yields

$$\frac{R}{B} = \frac{1.443}{C} [1-g(y)] \ln \left[\frac{C-(1-y)(1-g(y))}{y(1-g(y))} \right] \quad (3.2.15)$$

where

$$C = \frac{1}{\gamma} \ln \frac{1}{P_e} .$$

The above expression has to be maximised with respect to y . This is a single variable un-constrained optimization problem. Fibonacci's method of optimization has been used to find the optimum value of R/B , corresponding to an optimum values of M and y .

The results have been exhibited graphically and discussed at the end of the chapter (Section 3.5).

3.3 Phase-Shift-Keying:

Multiphase PSK signaling waveform at the receiver has the form

$$s(t) = \sqrt{2S} \cos(w_c t + \phi) \quad (3.3.1)$$

where S is the received signal power and ϕ may have any value in the discrete set $(\frac{2\pi}{M})k$; $k = 0, 1, 2, \dots, M-1$.

The total received signal at the receiver has the form

$$\begin{aligned} r(t) &= s(t) + n(t) \\ &= \sqrt{2S} \cos(w_c t + \phi) + x(t) \cos(w_c t + \phi) \\ &\quad - y(t) \sin(w_c t + \phi) \end{aligned} \quad (3.3.2)$$

where x and y are low-pass noise components of $n(t)$ with zero mean and power $\overline{x^2} = \overline{y^2} = N$.

Our aim is to find the probability of error under optimum detection. As is evident from the discussions of Section 2.5.1, an error occurs if the phase of $r(t)$, θ , is distorted beyond the region $-\frac{\pi}{M} \leq \theta \leq \frac{\pi}{M}$ with the assumption that $\phi = 0$ has been transmitted.

The probability density function of θ is given by [25] as

$$r(\theta) = \frac{1}{2\pi} e^{-\frac{S}{N}} \left[1 + \sqrt{4\pi S/N} \cos \theta e^{\frac{S}{N} \cos^2 \theta} \frac{1}{\sqrt{2\pi}} \int_{-\infty}^{\sqrt{\frac{2S}{N}} \cos \theta} e^{-x^2/2} dx \right] \quad (3.3.3)$$

Hence the probability of error, P_e , is given by

$$P_e = 1 - \int_{-\pi/M}^{\pi/M} p(\theta) d\theta \quad (3.3.4)$$

The equation (3.3.4) by using (3.3.3) can be expressed in closed form only for $M=2$ and 4. However an approximation valid for high SNR's given in [2] is sufficient for our purposes. Hence the probability of error under coherent optimum detection, P_{ec} , is given by

$$P_{ec} \approx e^{-\gamma} \sin^2 \pi/M \quad (3.3.5)$$

where $\gamma = S/N = \text{SNR}$

Similarly it has been shown that if the signal is processed differentially, then at large SNRs, the probability of error, ' P_{ed} ', for differentially detected multi-phase FSK is given by [2] as

$$P_{ed} \approx e^{-2\gamma} \sin^2 \pi/2M \quad (3.3.6)$$

The only major difference between this signal set and FSK signal set is that here the bandwidth is independent of M . Hence ' M ' is immediately determined by error rate and SNR using either eqn. (3.3.5) or eqn. (3.3.6). However we can compare the efficiencies of the two systems operating at same error rates, SNR and bandwidth.

The bandwidth associated with PSK is given by

$$B = KN ; N = \frac{1}{T} \quad (3.3.7)$$

where K is a constant which varies between 1 and 1.5.

The data rate per unit bandwidth associated with this set of signal is given by

$$(R/B)_\phi = \frac{1.443 \ln M}{K} \quad (3.3.8)$$

For fixed error rates and SNR M is determined either from eqn. (3.3.5) or eqn. (3.3.6). This ' M ' is then used in eqn. (3.3.8) to calculate $(R/B)_\phi$.

The results have been shown graphically for both, coherent as well as for differential PSK in Section 3.5.

3.4 Linear Modulation:

An exact probability of error calculations for multi-level amplitude modulation (AM) in additive white Gaussian noise with a spectral density of N_0 has been carried out in [2]. The probability of error ' P_{ea} ', is given by

$$P_{ea} = \left(1 - \frac{1}{M}\right) \operatorname{erfc} \left[\left(\frac{3\gamma}{M^2 - 1} \right)^{1/2} \right] \quad (3.4.1)$$

where M = number of levels

$$\gamma = \frac{P_s T}{N_0} = \text{SNR}$$

P_s = Transmitted power

T = bit duration

The bandwidth occupied by multi-level AM is

$$B = K' N, \quad N = \frac{1}{T} \quad (3.4.2)$$

where $K' = 1/2$ for single-side band (SSB) AM and $K' = 1$ for double side band (DSB) AM. In any practical linear modulation system $\frac{1}{2} \leq K' \leq 1$.

The data rate per unit bandwidth, in this case, is given by

$$(R/B)_a = \frac{1.443 \ln M}{K'} \quad (3.4.3)$$

The data rate per unit bandwidth calculations has been carried out for (a) SSS-AM and (b) DSB-AM. Here also we determine the value of M from Eqn. (3.4.1) for fixed values of P_e and SNR and use this value of M into Eqn. (3.4.3) to calculate the data rate per unit bandwidth. Care has been taken while calculating the value of M from eqn. (3.4.1) in case of SSB-AM because the value of SNR used must be

half to that of DSB-AM SNR. This is due to the fact that average SNR requirement of SSB-AM is half to that of DSB-AM.

Finally all these results are compared with Shannon's capacity theorem which states that for additive band-limited Gaussian channel, the maximum bits per cycle achievable is given by

$$(R/B)_s = 1.443 \ln (1 + \gamma) \quad (3.4.4)$$

while the probability of error is vanishingly small.

3.5 Results and Conclusions:

The numerical results have been shown in Tables 3.1 to 3.5.

Conclusions:

Figure 3.1 exhibits data rate per unit bandwidth versus SNR , γ , achievable for various systems. It is seen that most efficient system in terms of achieving data rate per unit bandwidth for fixed error rates and SNR is SSB-AM. It has the same slope as capacity curve. This is because the SSB-AM system has the least bandwidth occupancy and, therefore, can pump signals faster than any other systems. The data rate is directly proportional to the signaling rate and

Table 3.1

Data Rates at Various SNRs for FSK Optimum detection

SNR γ (dB)	$P_e = 10^{-6}$			$P_e = 10^{-8}$		
	Optimum	R/B	B/N	Optimum	R/B	B/N
	levels 'M'	Bits/S/Hz		levels 'M'	Bits/S/Hz	
10	6.478	1.005	2.683	7.638	0.920	3.190
15	7.803	1.338	2.215	7.380	1.252	2.303
20	10.061	1.708	1.950	9.404	1.612	2.007
25	13.454	2.123	1.766	12.471	2.015	1.807
30	18.551	2.585	1.631	17.082	2.465	1.661
35	26.192	3.088	1.526	24.017	2.959	1.550
40	38.049	3.630	1.446	34.745	3.492	1.446

Table 3.2

Data Rates at Various SNRs for PSK Coherent Detection

SNR γ (dB)	$P_e = 10^{-6}$				$P_e = 10^{-8}$			
	No. of levels 'M'	Data Rate, (R/B) ϕ			No. of levels 'M'	Data Rate, (R/B) ϕ		
		K=1	K=1.2	K=1.5		K=1	K=1.2	K=1.5
13	3.20	1.68	1.40	1.12	2.44	1.28	1.07	0.86
15	4.35	2.12	1.77	1.41	3.62	1.86	1.55	1.24
20	8.25	3.05	2.54	2.03	7.08	2.83	2.35	1.88
25	14.93	3.90	3.25	2.60	12.89	3.69	3.07	2.46
30	26.68	4.74	3.95	3.16	23.08	4.53	3.77	3.02
35	37.51	5.57	4.64	3.71	41.14	5.36	4.47	3.58
40	84.53	6.40	5.34	4.27	73.20	6.20	5.16	4.13

Table 3.3

Data Rates at Various SNRs for PSK Differential Detection

SNR γ (dB)	No. of levels 'M'	$P_e = 10^{-6}$			No. of levels 'M'	$P_e = 10^{-8}$		
		Data Rate, (R/B) \emptyset				Data Rate, (R/B) \emptyset		
		K=1	K=1.2	K=1.5		K=1	K=1.2	K=1.5
13	2.50	1.32	1.10	0.88	2.10	1.07	0.89	0.72
15	3.23	1.69	1.41	1.13	2.76	1.46	1.22	0.98
20	5.91	2.56	2.14	1.71	5.10	2.35	1.96	1.57
25	10.59	3.41	2.84	2.27	9.16	3.20	2.66	2.13
30	18.89	4.24	3.53	2.83	16.35	4.03	3.36	2.69
35	33.61	5.07	4.23	3.38	29.10	4.86	4.05	3.24
40	59.78	5.90	4.92	3.94	51.77	5.70	4.75	3.80

Table 3.4

Data Rates at Various SNRs for SSB-SC-AM

SNR γ (dB)	$P_e = 10^{-6}, K' = .5$		$P_e = 10^{-8}, K' = .5$	
	No. of levels		No. of levels	
	'M'	Data rate (R/B) $_a$	'M'	Data rate (R/B) $_a$
15	2.27	2.37	2.00	2.00
20	3.72	3.79	3.21	3.37
25	6.42	5.36	5.56	4.92
30	11.28	6.99	9.64	6.54
35	19.97	8.64	17.05	8.19
40	35.45	10.30	32.26	9.84

Table 3.5

Data Rates at Various SNRs for DSB-SC-AM

SNR γ (dB)	$P_e = 10^{-6}, K' = 1.0$		$P_e = 10^{-8}, K' = 1.0$		Shanon's capacity (R/B) _s
	No. of levels 'M'	Data rate (R/B) _a	No. of levels 'M'	Data rate (R/B) _a	
15	3.03	1.60	2.63	1.40	3.46
20	5.15	2.36	4.42	2.14	5.03
25	9.00	3.17	7.70	2.94	6.66
30	15.40	3.99	13.58	3.76	8.31
35	28.21	4.82	24.08	4.59	9.97
40	50.11	5.65	42.77	5.42	11.63

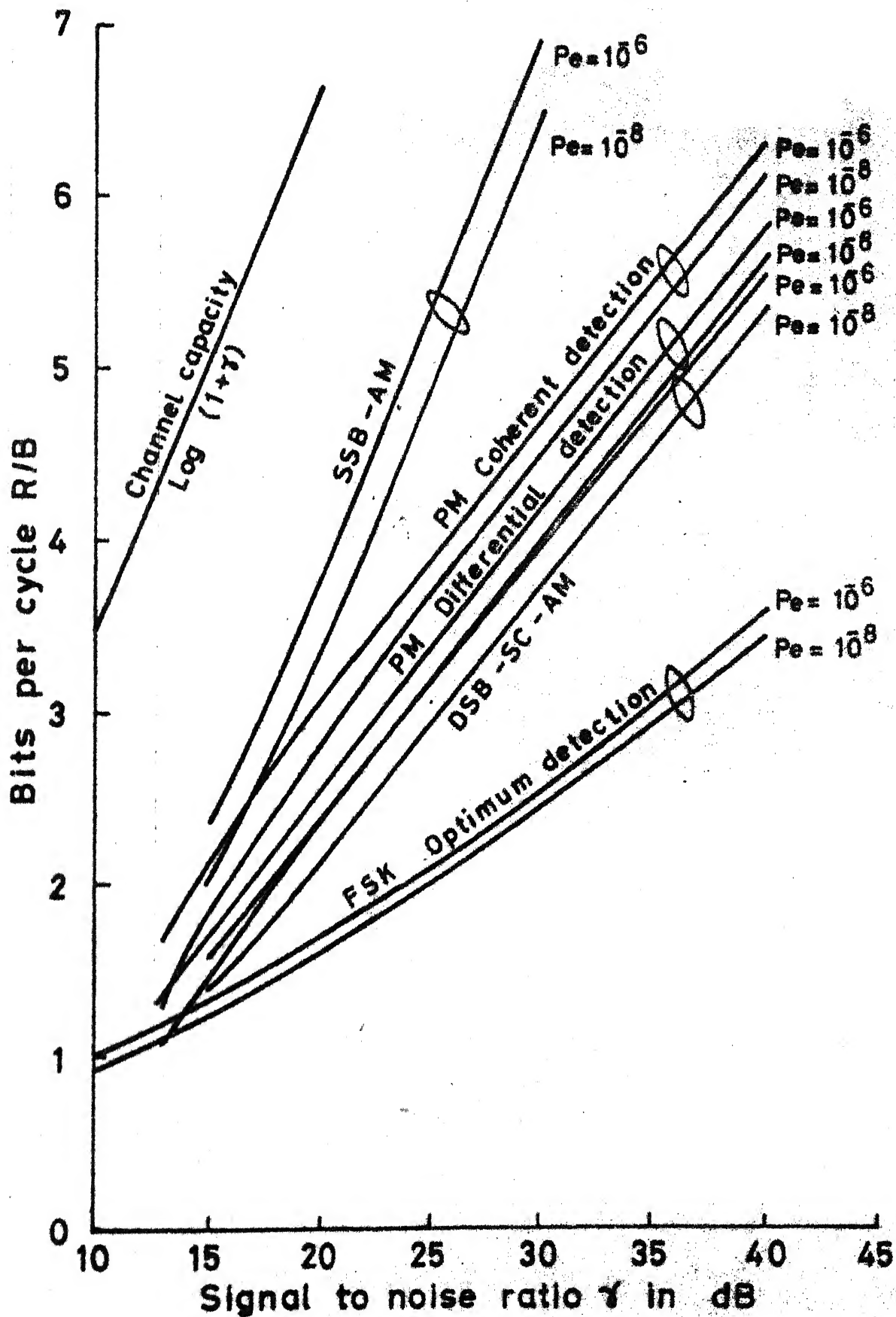
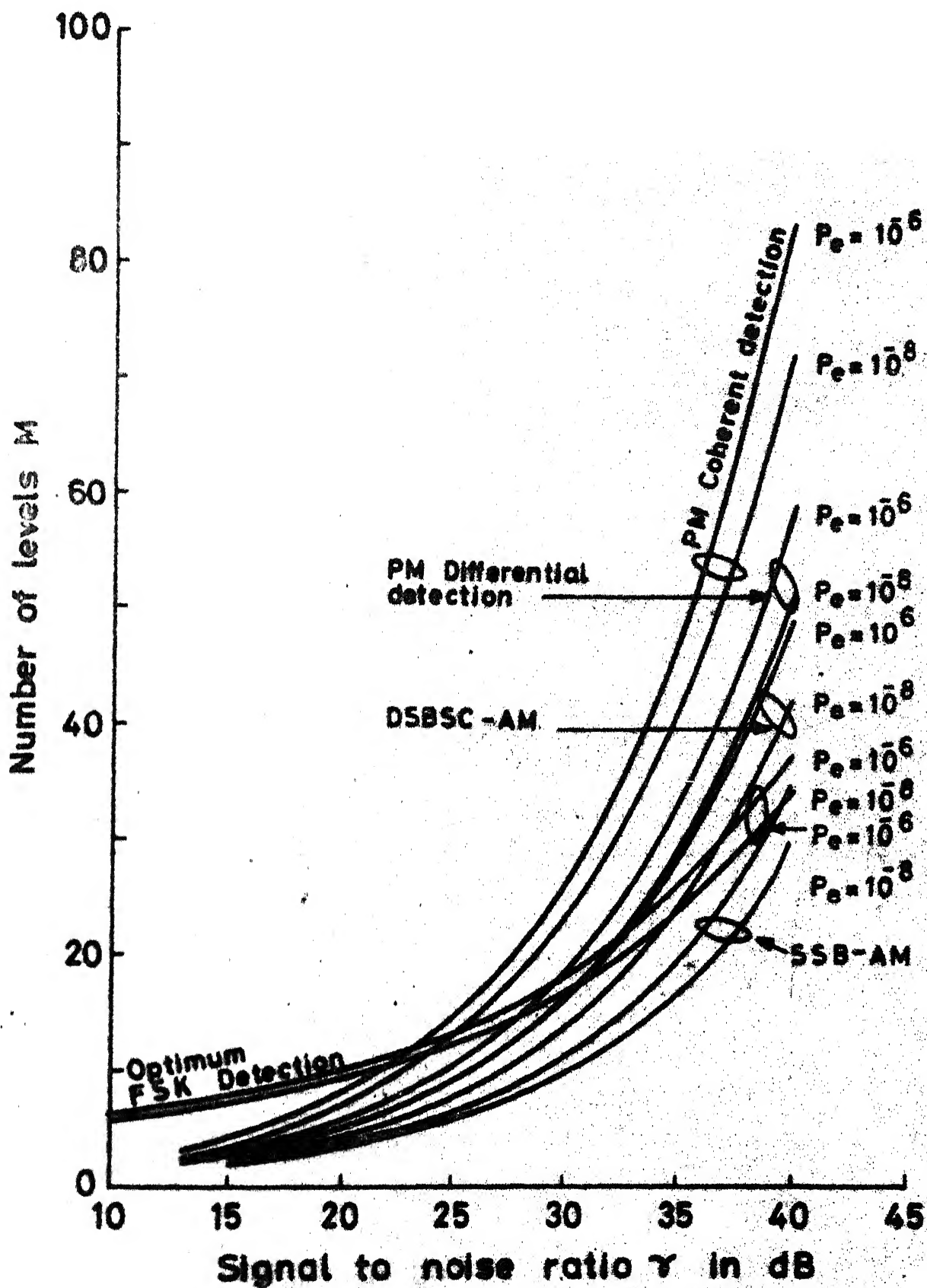
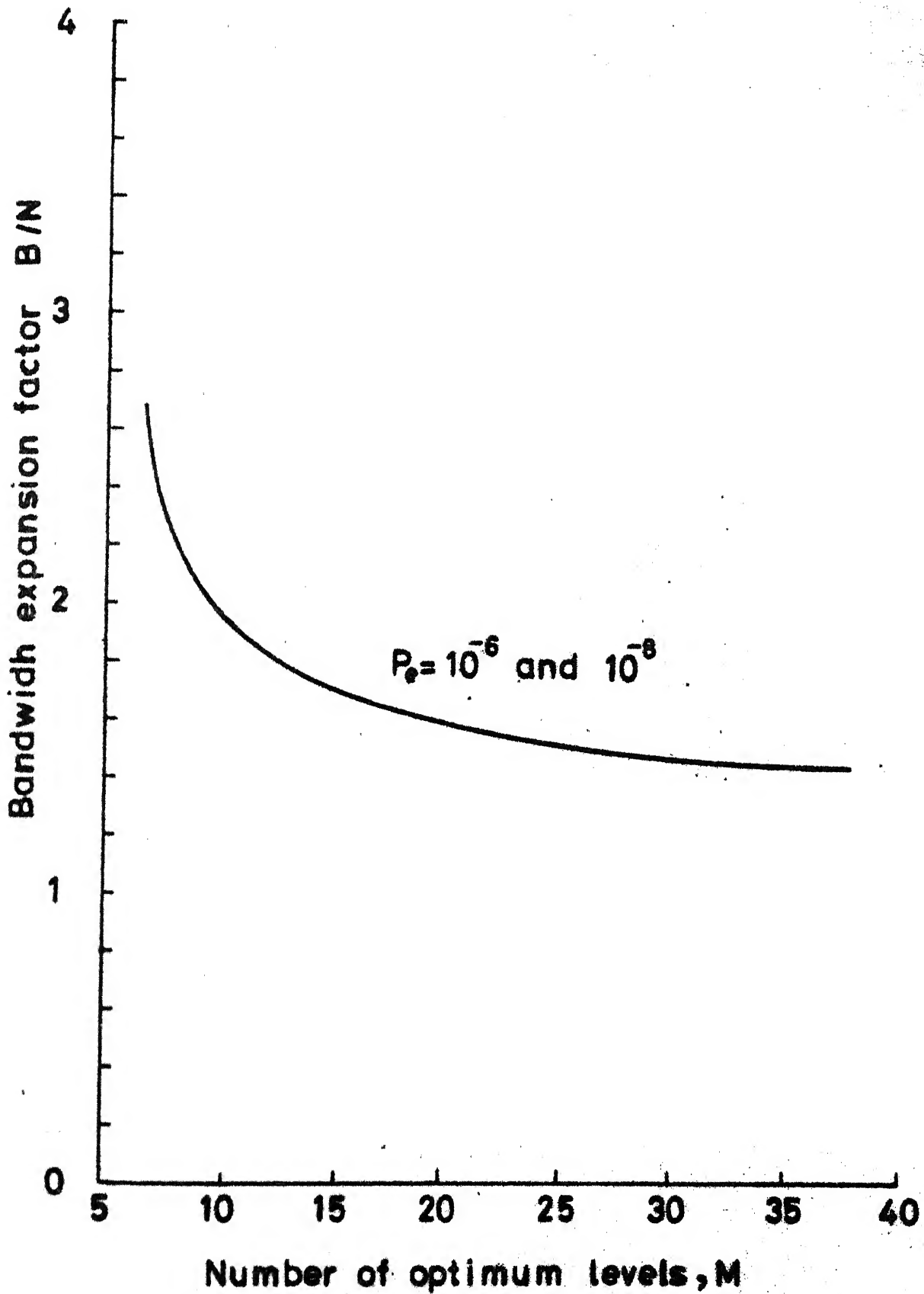


Fig. 3.1 Data rate comparison of systems (R/B vs SNR)



3.2 Number of levels M vs SNR for various systems



3.3 Bandwidth expansion factor B/N vs number of optimum levels M in FSK

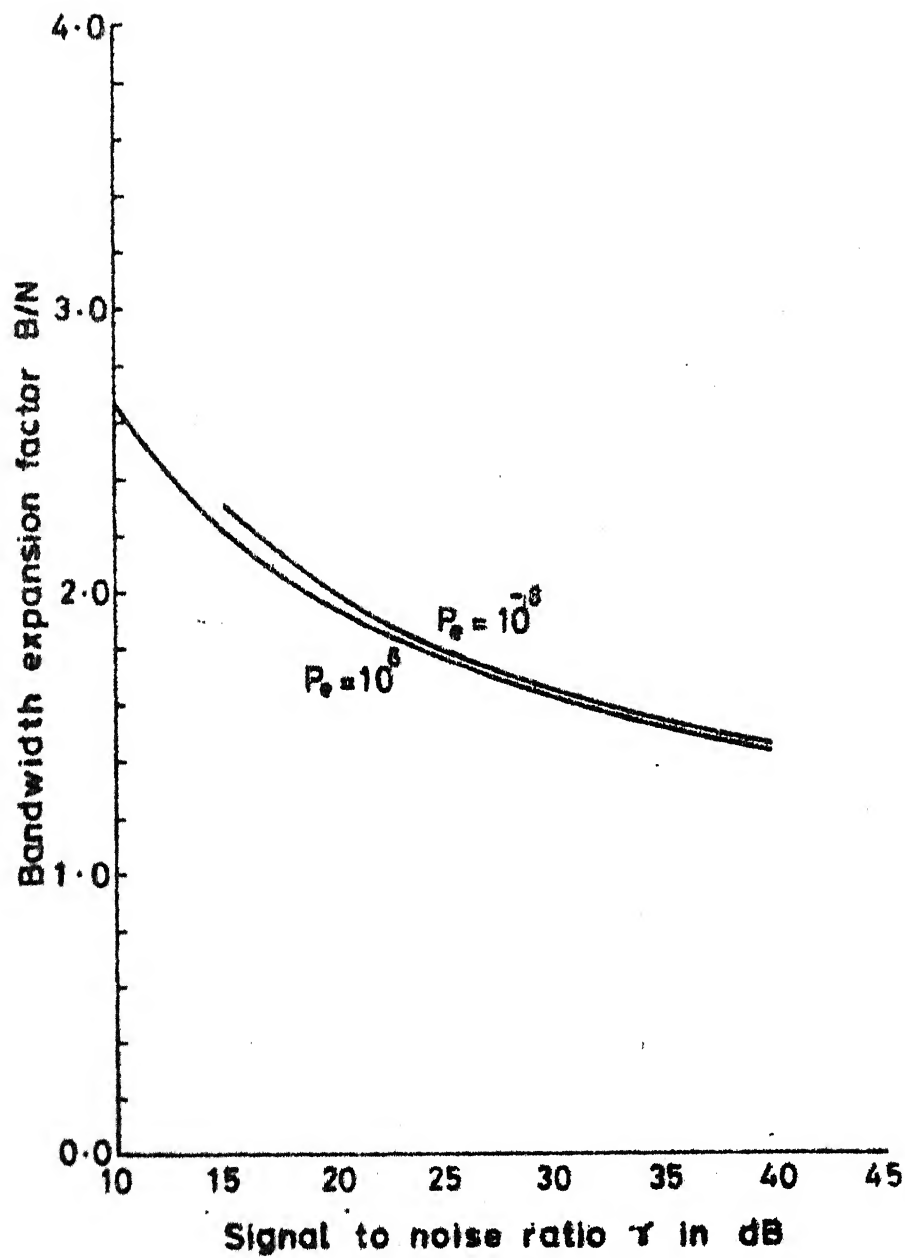


Fig. 3.4 Bandwidth expansion factor B/N vs SNR for optimised FSK

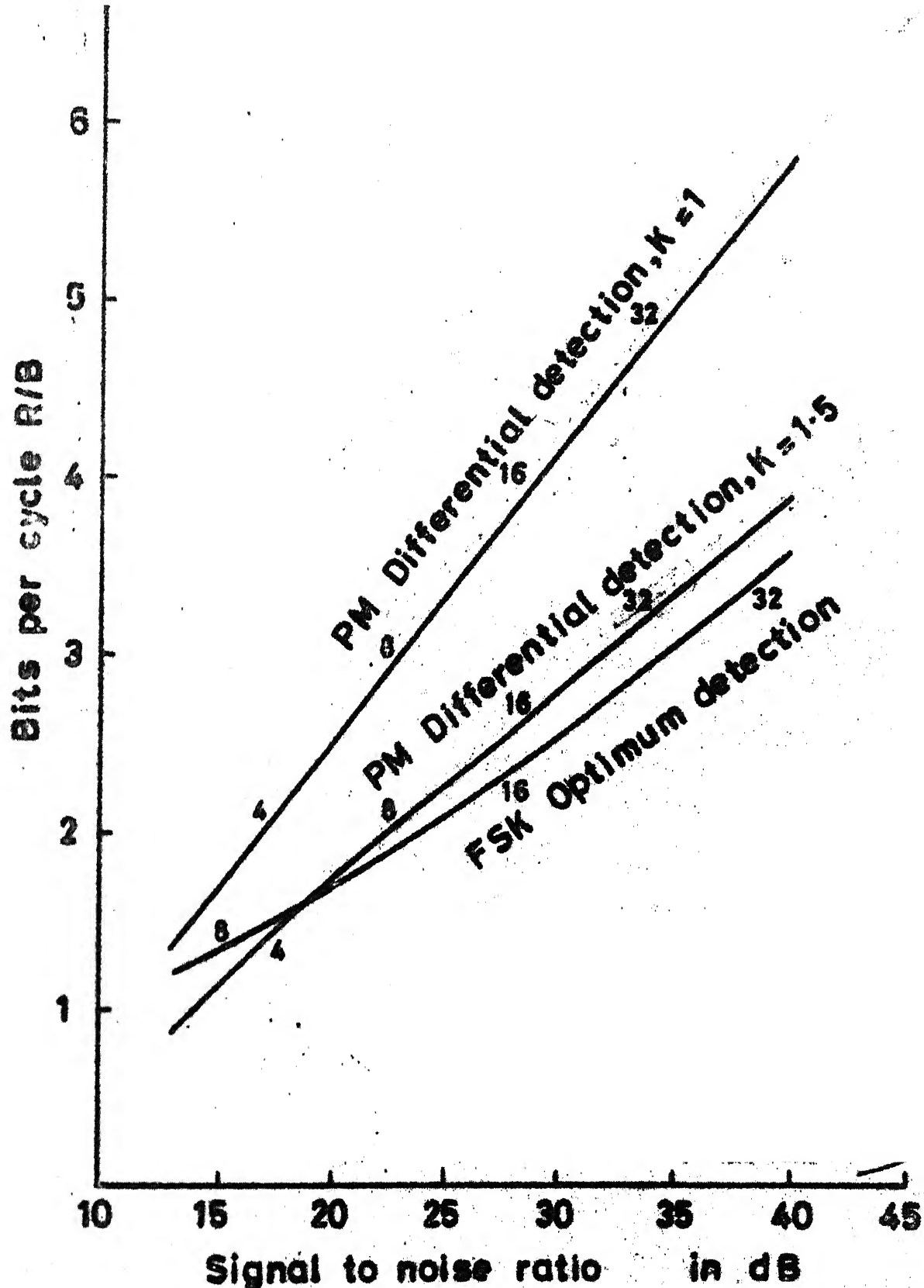
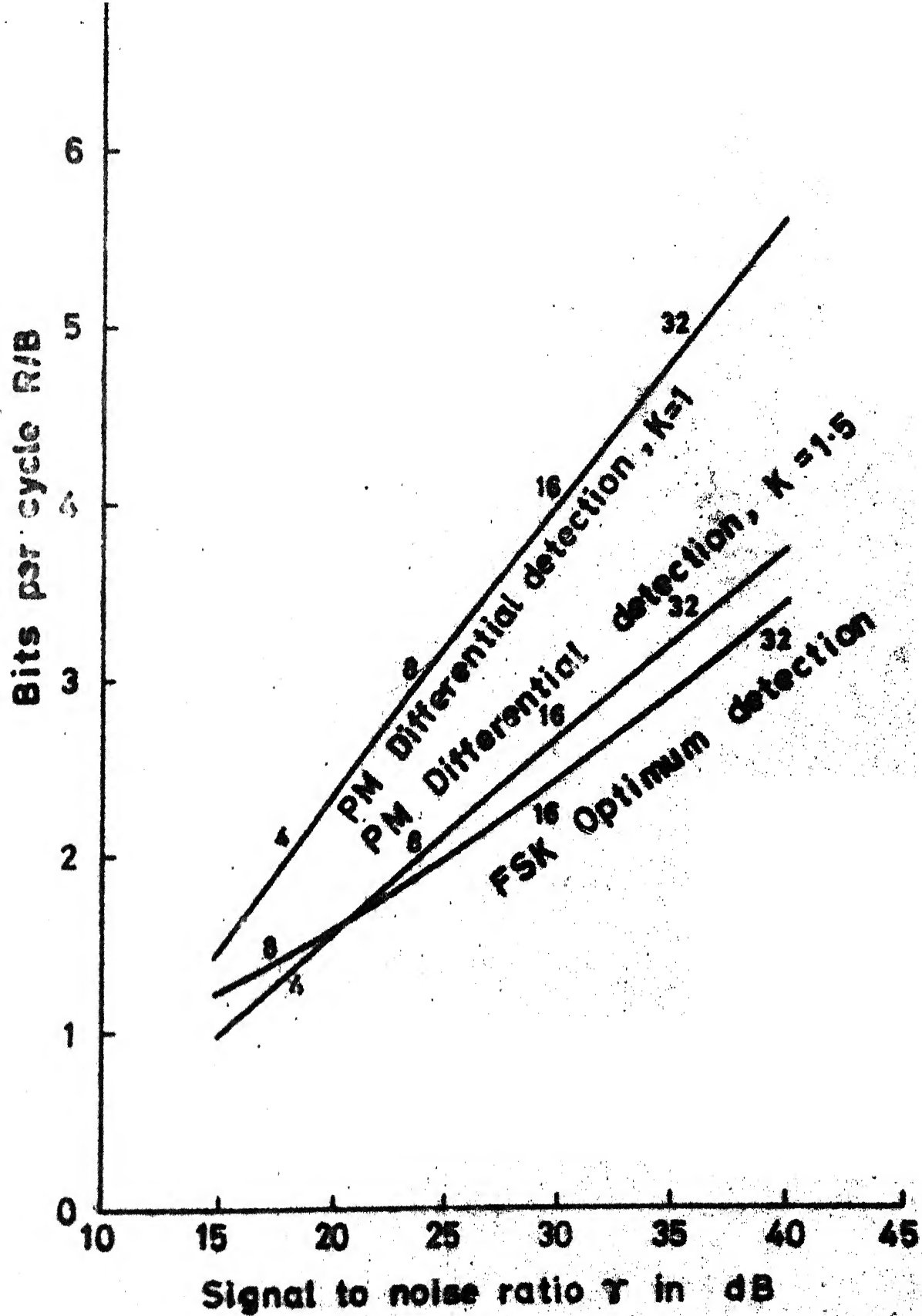


Fig. 3.5 Bit per cycle R/B vs SNR for optimised FSK and differential PM at $P_e = 10^{-6}$



3.6 Bits per cycle R/B vs SNR γ for optimised FSK and differential PM at 10^{-8}

also it varies logarithmically with the number of levels, therefore, system occupying greater bandwidth must increase their number of levels exponentially to achieve an identical data rate. This in turn forces the slower signaling rate systems to increase their SNR in order to keep the probability of error constant.

At large SNRs, the FM optimum system is the most inefficient. At $\text{SNR} < 12 \text{ dB}$, the differences are not that pronounced. The PM curves lie between SSB-AM and FM. This is due to the fact PM systems can utilise available bandwidth more efficiently than FM, yet not as efficiently as SSB-AM. The slope differential of SSB-AM and DSB-AM is a factor of 2. This is simply because the SSB-AM systems are twice as fast as DSBSC-AM systems. Since FM is also a DSB-system, it follows the same slope as DSB-AM, irrespective of detection mode. To achieve greater efficiency than SSB-AM, coding must be employed.

Figure 3.2 shows the number of levels M , or number of signals versus the SNR required to maintain a fixed probability of error for various systems considered. The number of levels associated with FSK systems are those which maximise the data rate per unit bandwidth. The fact that so many cross-error points occur, is attributed to the different way in which SNR varies with number of levels, so

as to maintain fixed error rate (in the respective systems). In AM and FM, $\gamma \sim M^2$ but in FSK $\gamma \sim M^\alpha$ where $\alpha > 2$. This accounts for the sharper rise in 'M' for large SNR in FM systems.

Figure 3.3 shows a plot between B/N (bandwidth expansion factor) versus optimum number of levels for FSK system. It is seen that behaviour of B/N is independent of error rates and $B/N \propto \left(\frac{1}{M}\right)^\theta$; $\theta > 0$. This explains the greater rise of 'M' with SNR in FSK as compared to FM and AM systems at large SNR's.

B/N is a most important parameter in FSK. It is a measure of how much more bandwidth than that of base-band is consumed. A graph is plotted in Figure 3.4, between B/N versus SNR for two different error rates (10^{-6} , 10^{-8}). The range of variations is surprisingly small. At large SNR, $B/N \approx 1.5$ while at $\gamma \approx 10$ dB, $B/N \approx 2.5$.

Differential PM is a system most closely resembling FM. The two graphs in Figures 3.1 and 3.2 assume a bandwidth equal to signaling rate, N. But practical PM systems may require a greater bandwidth than N. In Figures 3.5 and 3.6, plot of efficiency of differentially coherent PM using bandwidth equal to KN, for $K=1$ and $K=1.5$ versus SNR (γ) is

given. On these curves number of levels required to achieve efficiencies is shown at certain SNRs. On the same figures optimised FSK curves have also been plotted. The plots have been made for two different probability of errors i.e. in Figure 3.5, $P_e = 10^{-6}$ and in Figure 3.6, $P_e = 10^{-8}$. Due to various approximations made for mathematical simplicity, data SNR < 12 dB at $P_e = 10^{-6}$ and SNR < 15 dB for $P_e = 10^{-8}$ may not be reliable. It is interesting to note that there is not much of difference in the efficiencies of FSK system and FSK system, occupying a BW = $1.5 N$. A practical PM system can probably be designed to operate at $B=KN$, where $1 < K < 1.5$. This would indicate that DPSK is more efficient than FM at large SNRs.

CHAPTER 4

PERFORMANCE OF SYSTEMS UNDER RAYLEIGH FADING

4.1 INTRODUCTION:

Till now we have discussed the performances of various digital modulation schemes under ideal conditions only. In this chapter, we shall study the effect of fading on the performances of these schemes.

In practical situations, the changing nature of the communication medium, for example ionosphere, causes the received signals to fade. Without going into mechanisms of fading, we shall assume that probability density function (pdf) of the fading envelope is that of Rayleigh[5].

We carry out identical studies analogous to that done in Chapter 2. Under the assumption of ^{Rayleigh} behaviour of the channel, probabilities of errors are calculated. In doing so, we assume that the fading is non-selective. For simplicity in arriving at results, we shall assume that ISI is zero. As before, we consider that the channel introduces only additive white Gaussian noise. In our study, we have confined ourselves to slow fading only.

4.2.1 OOK: Non-coherent detection[5]

Under the assumption that a '1' (Mark) is transmitted, the envelope of signal, u , at the filter at the sampling

interval is a random variable with a Rayleigh pdf given by

$$f(u) = \frac{2u}{u_0^2} e^{-\frac{u^2}{u_0^2}} ; 0 \leq u < \infty \quad (4.2.1)$$

where

$u_0^2 = E[u^2]$ is the mean square value of u averaged over the entire fading range. The filter output noise intensity at every sampling instant is still N , unchanged from pulse to pulse. Hence SNR at sampling instant is given as

$$= \frac{u^2}{2N} \quad (4.2.2)$$

Hence γ is a random variable from pulse to pulse. With equation (4.2.1) and u as a constant, pdf of γ is the exponential distribution.

$$p(\gamma) = \frac{1}{\gamma_0} e^{-\frac{\gamma}{\gamma_0}} ; 0 \leq \gamma < \infty \quad (4.2.3)$$

where

$$\gamma_0 = E[\gamma] = \frac{u_0^2}{2N} \quad (4.2.4)$$

For a fixed threshold 'b' normalised to N as

$$b_0 = \frac{b}{\sqrt{N}} \quad (4.2.5)$$

the conditional probability of error for each decision is given by

$$P_e(\gamma) = \frac{1}{2} \left[1 - Q(\sqrt{2}\gamma, b_0) \right] + \frac{1}{2} e^{-b_0^2/2} \quad (4.2.6)$$

Therefore the average probability of error is given by

$$P_e = \int_0^{\infty} P_e(\gamma) p(\gamma) d\gamma \quad (4.2.7)$$

Substituting the values of $P_e(\gamma)$ and $p(\gamma)$ into equation (4.2.7) and carrying out the integration we get,

$$P_e = \frac{1}{2} \left[1 - \exp(-b_0^2/2 \cdot \frac{1}{1+\gamma_0}) \right] + \frac{1}{2} \exp(-b_0^2/2) \quad (4.2.8)$$

The optimum threshold, b_0 , can be found by differentiating equation (4.2.8) with respect to b_0 and equating it to zero. This yields

$$\hat{b}_0 = \sqrt{2(1 + \frac{1}{\gamma_0}) \ln(1 + \gamma_0)} \quad (4.2.9)$$

At large SNRs and under the optimum threshold,

$$P_e \propto \frac{1}{2} \frac{\ln \gamma_0}{\gamma_0} \quad (4.2.10)$$

With Rayleigh fading covering the entire range of values $(0, \infty)$, no fixed threshold can properly discriminate signals (Mark) from noise (space) over variety of levels. Therefore, under the assumption of sufficiently slow fading,

one might consider the possibility of continuously adjusting the threshold at each instant to the optimum value (minimum probability of error) corresponding to the fading level at that instant. Then P_e is given by equation (4.2.7) where $P_e(\gamma)$ is given by equation (4.2.6) and b_0 is to be obtained from

$$e^{-\gamma} I_0(b_0 \sqrt{2\gamma}) = 1 \quad (4.2.11)$$

At high SNRs, see equation (2.2.8)

$$b_0 \approx \sqrt{\gamma/2}$$

For this value of b_0 it has been shown [5] that the curve of P_e versus SNR (γ_0) approaches

$$P_e \approx \frac{1.63}{\gamma_0} \quad (4.2.12)$$

SNR calculations:

Optimum fixed threshold:

Using equation (4.2.10) we get for

$$P_e = 10^{-2}, \quad \gamma_0 = 21.6 \text{ dB}$$

$$\text{and for } P_e = 10^{-4}, \quad \gamma_0 = 44.35 \text{ dB}$$

Optimum variable threshold:

Using equation (4.2.12), we get

$$\text{for } P_e = 10^{-2}, \quad \gamma_0 = 19.1 \text{ dB}$$

$$\text{and for } P_e = 10^{-4}, \quad \gamma_0 = 39.1 \text{ dB}$$

Comparing the figures for SNRs in case of optimum fixed threshold and optimum variable threshold in OOK non-coherent scheme, it is found that latter has an advantage of 2.5 dB at $P_e = 10^{-2}$ and 5.25 dB at $P_e = 10^{-4}$.

4.2.3 OOK: Coherent detection [5]

Since optimum variable threshold gives a better performance than optimum fixed threshold, we shall discuss only the former for the coherent case, here.

The conditional probability of error dependent on γ in case of coherent OOK detection is given by equation (2.2.4) as

$$P_e(\gamma) = \frac{1}{2} \operatorname{erfc}(\sqrt{\gamma}/2) \quad (4.2.12)$$

Hence average probability of error is ^{given} by equation (4.2.7). Substituting the values of $P_e(\gamma)$ and $p(\gamma)$ from equations (4.2.12) and (4.2.3) into equation (4.2.7) respectively and solving, we get

$$P_e = \frac{1}{2} \left(1 - \frac{1}{\sqrt{1+4/\gamma_0}} \right) \quad (4.2.13)$$

At high SNRs,

$$P_e \approx \frac{1}{\gamma_0} \quad (4.2.14)$$

SNRs per bit required to achieve various bit error rates have been shown in Table 4.2.

4.3.1 BFSK: Coherent detection [5]

The conditional probability of error for BFSK coherent detection is given by equation (2.3.2) as

$$P_e(\gamma) = \frac{1}{2} \operatorname{erfc}(\sqrt{\gamma/2}) \quad (4.3.1)$$

Substituting the values of $P_e(\gamma)$ and $p(\gamma)$ from equations (4.3.1) and (4.2.3) respectively into equation (4.2.7) and solving, we get the average probability of error, P_e , as

$$P_e = \frac{1}{2} \left(1 - \frac{1}{\sqrt{1 + \frac{1}{\gamma_0}}} \right) \quad (4.3.2)$$

At high SNR,

$$P_e \approx \frac{1}{2\gamma_0} \quad (4.3.3)$$

SNRs per bit required to achieve various bit error rates have been shown in Table 4.2.

4.3.2 BFSK: Non-coherent detection [5]

Here the conditional probability of error is given by equation (2.3.3) as

$$P_e(\gamma) = \frac{1}{2} e^{-\gamma/2} \quad (4.3.4)$$

Substituting the values of $P_e(\gamma)$ and $p(\gamma)$ from equations (4.3.4) and (4.2.3) into equation (4.2.7) respectively and solving, we get

$$P_e = \frac{1}{2 + \gamma_0} \quad (4.3.5)$$

At high SNRs,

$$P_e \propto \frac{1}{\gamma_0} \quad (4.3.6)$$

SNRs per bit required to achieve various bit error rates have been shown in Table 4.2.

4.4.1 BPSK: Ideal coherent detection [5]

The conditional probability of error is given by equation (2.4.2) as,

$$P_e(\gamma) = \frac{1}{2} \operatorname{erfc}(\sqrt{\gamma}) \quad (4.4.1)$$

Substituting the above value of $P_e(\gamma)$ and the value of $p(\gamma)$ from equation (4.2.3) into equation (4.2.7) and carrying out the integration, one gets

$$P_e = \frac{1}{2} \left(1 - \frac{1}{\sqrt{1 + \frac{1}{\gamma_0}}} \right) \quad (4.4.2)$$

At high SNRs,

$$P_e \propto \frac{1}{4 \gamma_0} \quad (4.4.3)$$

SNRs per bit required to achieve various bit error rates have been shown in Table 4.2.

4.4.2 DPSK [5] :

Here $P_e(\gamma)$ is given by equation (2.4.3) as

$$P_e(\gamma) = \frac{1}{2} e^{-\gamma} \quad (4.4.4)$$

The average probability of error is then obtained by solving equation (4.2.7) by using the values of $P_e(\gamma)$ and $p(\gamma)$ from equations (4.4.4) and (4.2.3) respectively and is given by

$$P_e = \frac{1}{2+2\gamma_0} \quad (4.4.5)$$

At high SNR,

$$P_e \approx \frac{1}{2\gamma_0} \quad (4.4.6)$$

SNRs per bit required to achieve various bit error rates have been shown in Table 4.2.

4.5 MSK(h = .5) and OK-QPSK:

Under the assumption of Chapter 2.6, the average bit probability of error in case of MSK and OK-QPSK would be same ^{as} BPSK coherent detection under Rayleigh-fading.

4.6.1 Multiphase PSK: coherent detection [20]

The PSK signal-suffering from slow fading can be written as

$$\begin{aligned} s(t) &= R(t) \cos [w_c t + \psi(t) + \phi(t)] \\ &= R(t) \cos [w_c t + \lambda(t)] \end{aligned} \quad (4.6.1)$$

where

w_c = angular carrier frequency

$R(t)$ = fading envelope

$\psi(t)$ = random phase due to fading

$\phi(t)$ = digital phase modulating signal.

Let the noise, $n(t)$, be AWGN then,

$$n(t) = x(t) \cos [w_c t + \lambda(t)] - y(t) \sin [w_c t + \lambda(t)] \quad (4.6.2)$$

where $x(t)$ and $y(t)$ are in phase and quadrature components of $n(t)$. Then, the input to detector is given by

$$s(t) + n(t) = \sqrt{[R(t) + x(t)]^2 + y^2(t)} \cos [w_c t + \lambda(t) + \theta(t)] \quad (4.6.3)$$

$$\text{where } \theta(t) = \tan^{-1} \frac{y(t)}{R(t) + x(t)} ; \quad -\pi \leq \theta \leq \pi \quad (4.6.4)$$

For a coherent detection scheme with $\psi(t)$ as reference phase

available, the output from the detector can be written as

$$\phi^*(t) = \lambda(t) + \theta(t) - \psi(t) = \phi(t) + \theta(t) \quad (4.6.5)$$

Hence the detection error is dependent on $\theta(t)$ i.e. the composite phase of signal and noise given by equation (4.6.4).

Characterization of $\theta(t)$ conditional on $R(t)$:

The conditional p.d.f. of θ conditional on R , $f(\theta/R)$, is given by equation (3.3.3) as

$$f(\theta/R) = \frac{e^{-R^2/2N}}{2\pi} + \frac{R \cos \theta}{2\sqrt{2\pi N}} e^{-R^2 \sin^2 \theta / 2N} \left[1 + \operatorname{erf} \left(\frac{R \cos \theta}{\sqrt{2N}} \right) \right] \quad (4.6.7)$$

where N is the noise power and $\operatorname{erf}(x) = \text{error function}$

$$= \frac{2}{\sqrt{\pi}} \int_0^x e^{-t^2} dt$$

The probability of error for M-phase PSK conditional on R is thus given by equation (3.3.4) as

$$P_e(R) = 1 - \int_{-\pi/M}^{\pi/M} f(\theta/R) d\theta \quad (4.6.8)$$

The pdf of fading envelope $R(t)$ is given as

$$p(R) = \frac{2R}{\Omega} e^{-R^2/\Omega} \quad (4.6.9)$$

where,

$\Omega = E[R^2]$ is the mean square value of R .

The average probability of error for M -phase PSK can now be written as

$$\begin{aligned} P_e &= \int_0^{\infty} P_e(R) p(R) dR \\ &= 1 - \int_{-\pi/M}^{\pi/M} p(\theta) d\theta \end{aligned} \quad (4.6.10)$$

where,

$$p(\theta) = \int_0^{\infty} f(\theta|R) p(R) dR \quad (4.6.11)$$

The value of $p(\theta)$ has been evaluated in closed form and is given by [20] as

$$p(\theta) = \frac{1}{2\pi} \left[\frac{\pi}{2} \frac{\sqrt{\gamma_0} \cos \theta}{(1 + \sqrt{\gamma_0} \sin^2 \theta)^{3/2}} + \frac{1}{(1 + \gamma_0)} F\left(1, 1, \frac{1}{2}; \frac{\gamma_0 \cos^2 \theta}{1 + \gamma_0}\right) \right] \quad (4.6.12)$$

where

$\gamma_0 = \frac{\Omega}{2N}$ = mean SNR and $F(.,.,.,.;.)$ is the hypergeometric function defined as

$$F(\alpha, \beta, \gamma; Z) = \sum_{n=0}^{\infty} \frac{(\alpha)_n (\beta)_n}{(\gamma)_n} \frac{Z^n}{n!} \quad (4.6.13)$$

Table 4.1

Probability of error for multiphase PSK

SNR γ_o dB	Probability of error P_e			
	$M = 2$	$M = 4$	$M = 8$	$M = 16$
0	1.464×10^{-1}	3.650×10^{-1}	6.153×10^{-1}	7.950×10^{-1}
5	6.418×10^{-2}	1.932×10^{-1}	4.260×10^{-1}	6.666×10^{-1}
10	2.326×10^{-2}	7.857×10^{-2}	2.251×10^{-1}	4.729×10^{-1}
15	7.723×10^{-3}	2.788×10^{-2}	9.180×10^{-2}	2.603×10^{-1}
20	2.481×10^{-3}	8.949×10^{-3}	3.206×10^{-2}	1.098×10^{-1}
25	7.886×10^{-4}	2.860×10^{-3}	1.049×10^{-2}	3.905×10^{-2}
30	2.498×10^{-4}	9.077×10^{-4}	3.354×10^{-3}	1.286×10^{-2}
35	7.903×10^{-5}	2.873×10^{-4}	1.064×10^{-3}	4.121×10^{-3}
40	2.499×10^{-5}	9.090×10^{-5}	3.369×10^{-4}	1.309×10^{-3}
45	7.905×10^{-6}	2.875×10^{-5}	1.066×10^{-4}	4.145×10^{-4}
50	2.499×10^{-6}	9.093×10^{-6}	3.370×10^{-5}	1.311×10^{-4}
55	7.905×10^{-7}	2.877×10^{-6}	1.065×10^{-5}	4.146×10^{-5}
60	2.499×10^{-7}	9.137×10^{-7}	3.365×10^{-6}	1.311×10^{-5}

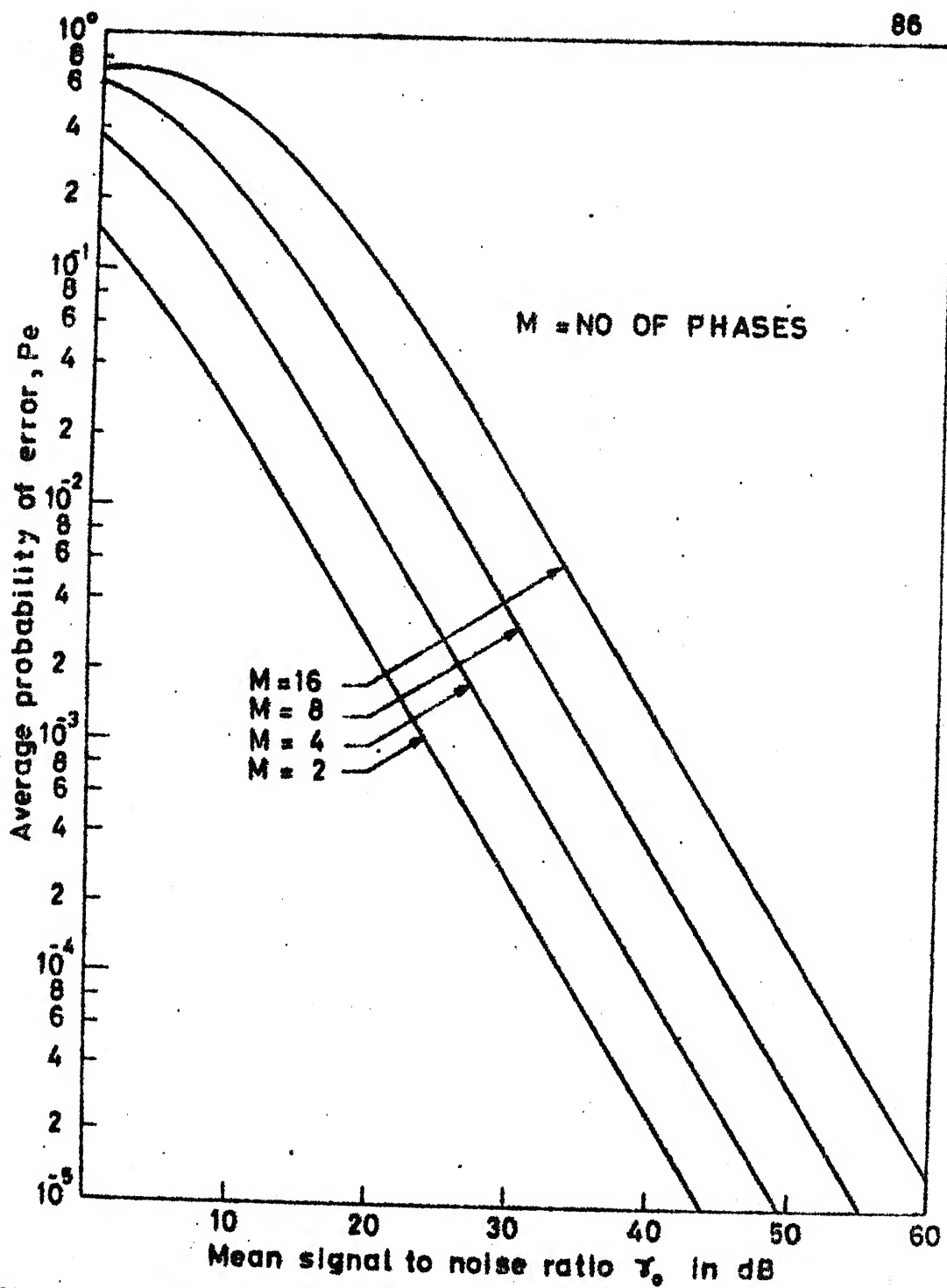


Fig. 4.1 Performance of multi-phase coherent PSK under Rayleigh fading

$$\text{now let } P(\phi) = \int_0^{\phi} p(\theta) d\theta ; 0 \leq \phi \leq \pi/2 \quad (4.6.14)$$

Then

$$P_e = 1 - 2 P(\pi/M) \quad (4.6.15)$$

The average probability of error, P_e , is now given [20] as

$$P_e = 1 - \frac{1}{\pi} \left[\frac{\pi}{M} + \frac{\sqrt{\gamma_0} \sin \pi/M}{\sqrt{1 + \gamma_0 \sin^2 \pi/M}} \left(\frac{\pi}{2} + \sin^{-1} \left(\sqrt{\frac{\gamma_0}{1 + \gamma_0}} \cos \pi/M \right) \right) \right] \quad (4.6.16)$$

Results:

A graph has been plotted in Figure 4.1 between P_e and the mean SNR γ_0 for $M=2, 4, 8$ and 16 . It is observed that the curves ^{become} straight lines at high SNRs.

For calculations of SNRs, the symbol error rates have been converted to bit error rates and symbol SNRs to bit SNRs. The actual values of bit SNRs required to achieve bit error rates of 10^{-2} and 10^{-4} have been shown in Table 4.2. The criterion used to convert symbol error rates to bit error rates and symbol SNRs to bit SNRs has been assumed to be same as in Chapter 2, Section 2.5. The values have been taken from the graph shown in Figure 4.1.

4.6.2 Multiphase PSK: Differential detections:

The exact evaluation of probability of error in case of M -ary DPSK in a closed form is not mathematically viable.

However, we can utilise the value of conditional probability of error $P_e(\gamma)$, given by equation (2.5.17) which is accurate at high SNR for calculation of average probability of error for M-ary DPSK case. $P_e(\gamma)$ is given as

$$P_e(\gamma) = \text{erfc}(\sqrt{2\gamma} \sin \pi/2M) \quad (4.6.17)$$

The average probability of error is then obtained by evaluating equation (4.2.7) by the help of equations (4.6.17) and (4.2.3) and is given by

$$P_e = 1 - \frac{1}{\sqrt{1 + \frac{1}{2 \gamma_0 \sin^2 \pi/2M}}} \quad (4.6.18)$$

At high SNRs,

$$P_e \approx \frac{1}{4 \gamma_0 \sin^2 \pi/2M} \quad (4.6.19)$$

For 4 phase PSK (DQPSK), above can be simplified as

$$P_e \approx \frac{1.707}{\gamma_0} \quad (4.6.20)$$

The SNRs per bit required to achieve bit errors rates of 10^{-2} and 10^{-4} have been shown in Table 4.2. The criterion used to convert symbol error rates to bit error rates and symbol SNRs to bit SNRs has been assumed to be same as in Chapter 2, Section 2.5.

4.7 Comparison of modulation schemes under the effect of Rayleigh fading:

Table 4.2

Performance of representative modulation schemes
on Raleigh fading channel

	Average mean SNR per bit γ_0 in dB ($P_e=10^{-2}$)	Average mean SNR per bit γ_0 in ($P_e=10^{-4}$)
OOK: coherent detection	17 *	37 *
OOK: Non-coherent detection	19.1 *	39.1 *
BFSK: coherent detection	20	40
BFSK: non-coherent detection	17	37
MSK($h = .5$)	14	34
BPSK	14	34
DPSK	17	37
QPSK	13.5	33.5
8-PSK	15.5	35.5
16-PSK	19	39
DQPSK	16.3	36.5
OK-QPSK	14	34

* Assumes variable optimum threshold.

Table 4.2 has been prepared to portray the significant differences in SNRs needed for various BERs under the effect of Rayleigh fading. Because of the severe effects of the fading, bit error rates (BERs) of 10^{-2} and 10^{-4} have been assumed for SNR calculations. The symbol error rates have been converted to bit error rates and SNRs required for various BERs have been converted to bit SNRs for comparison purposes. Comparing Tables 2.4 and 4.2, it is seen that values of Table 4.2 are weighted averages of ideal performance values. The relative performance of the scheme does not differ markedly from that indicated in Table 2.4. The effect of fading is so severe that to achieve a bit error rate of 10^{-4} in BPSK case, the SNR required is 34 dB; an increase of approximately 25.6 dB. No practical digital modulation scheme can afford either this increase in signal power or can work at error rate of 10^{-2} . This problem can be solved by using some techniques which reduce the effect of fading. Diversity combining techniques is one of the schemes. We shall very briefly discuss some diversity techniques in the next chapter.

CHAPTER 5

PERFORMANCE OF SYSTEMS UNDER LINEAR DIVERSITY COMBINING TECHNIQUES

5.1 INTRODUCTION

In the previous chapter, we have seen that severe degradation in the performance of digital systems caused by Rayleigh fading. The degradation is of the order of tens of decibels of SNR for the same bit error rates. To overcome this difficulty, one has to increase the transmitted power, antenna size etc. But any arbitrary increase of these parameters is severely constrained due to practical limitations and economic viability. As such any alternate technique which overcome (or diminish) the effect of fading is particularly attractive.

Diversity is one of such techniques which is commonly used. In practical situations, the transmitted signal arrives at the receiver via multiple paths (branch), the signals on each path containing a fraction of total transmitted power. Since fading does not degrade signals on all paths simultaneously, these multiple received signals can be combined and processed to overcome the effect of fading.

We shall confine ourselves with linear diversity combining techniques only where relatively simple weighted linear sum of multiple received signals are processed for decision making.

Our aim is to calculate the probability of error for various digital systems under diversity combining technique. Depending upon the combining techniques, the probability of error calculations will vary. The probability of error calculations have been carried out only for maximal ratio combining technique which is the most general case of linear combining techniques.

Maximal ratio combining:

Let $V_k(t)$ denote the total envelope of the signal corresponding to the k th path of the receiver. Then the most general linear combining results in an output given as

$$v(t) = \sum_{k=1}^M \alpha_k v_k(t) \quad (5.1.1)$$

where M is the number of diversity branches - and α_k are complex weighting factors which are changed according to the branch signals. These are called the combiner weighting factors. Selector combining is a particular case of maximal ratio combining where at any instant, all α_k are

zero except for the branch with largest SNR where it is some arbitrary constant. Selector combining involves transients due to switching [5]. Thus there are practical reasons for designing a combiner in which α_k vary more gradually with signal fading so that abrupt switching is avoided.

In equal gain combining technique, the weighting factors α_k have opposite phases to that of the signals in the respective branches, but all have equal magnitudes. Hence the name, equal gain combining. This method also provides an effective diversity performance. The performance here is definitely not as good as maximal ratio combining which requires a major effort in instrumentation to achieve the correct weighting factors, but good enough taking into account the simplicity in instrumentation.

Probability density function (pdf) of γ over short term fading for equal branch SNRs [5] :

Let γ_k denote the instantaneous signal to noise ratio in the k th receiver. Assuming Rayleigh pdf, one can write the pdf of γ_k as

$$p(\gamma_k) = \frac{1}{\Gamma_k} e^{-\gamma_k / \Gamma_k} \quad (5.1.2)$$

where $\Gamma_k = E[\gamma_k]$ is the average mean square SNR in the

kth receiver (branch). An optimal maximal ratio combining results in an instantaneous output SNR (γ) which is the sum of instantaneous SNRs on the individual branches. Thus

$$\gamma = \sum_{k=1}^M \gamma_k \quad (5.1.3)$$

Assuming γ_k to be independently and exponentially distributed and the fact that γ and γ_k are all positive real, pdf of γ is given by 5 as

$$p(\gamma) = \frac{1}{r^M} \frac{\gamma^{M-1}}{(M-1)!} e^{-\gamma/r} \quad (5.1.4)$$

where $r = r_k$.

We shall utilise equation (5.1.4) for the calculation of probability of error for various digital systems. Our approach in calculating the probability of error is same as that adopted in previous chapter.

5.2.1 BFSK: Coherent detection [5]

The probability of error given by equation (2.3.2) is now conditional on γ and can be written as

$$P_e(\gamma) = \frac{1}{2} \operatorname{erfc}(\sqrt{\gamma/2}) \quad (5.2.1)$$

Therefore the average probability of error can be obtained by averaging $P_e(\gamma)$ over the entire range of $\gamma(0, \infty)$.

Table 5.1

Probabilities of errors at various SNRs for FSK:
coherent detection

SNR Γ (dB)	Probability of error, P_e	
	No. of diversity branches (M)=2	No. of diversity branches (M)=4
0	1.138×10^{-1}	3.985×10^{-2}
2	7.441×10^{-2}	2.109×10^{-2}
4	4.317×10^{-2}	7.676×10^{-3}
6	2.350×10^{-2}	2.222×10^{-3}
8	1.173×10^{-2}	5.876×10^{-4}
10	5.476×10^{-3}	1.329×10^{-4}
12	2.427×10^{-3}	2.657×10^{-5}
14	1.037×10^{-3}	4.893×10^{-6}
16	4.327×10^{-4}	8.541×10^{-7}
18	1.775×10^{-4}	1.440×10^{-7}
20	7.203×10^{-5}	2.373×10^{-8}
22	2.902×10^{-5}	3.857×10^{-9}
24	1.164×10^{-5}	6.210×10^{-10}
25	7.368×10^{-6}	2.486×10^{-10}

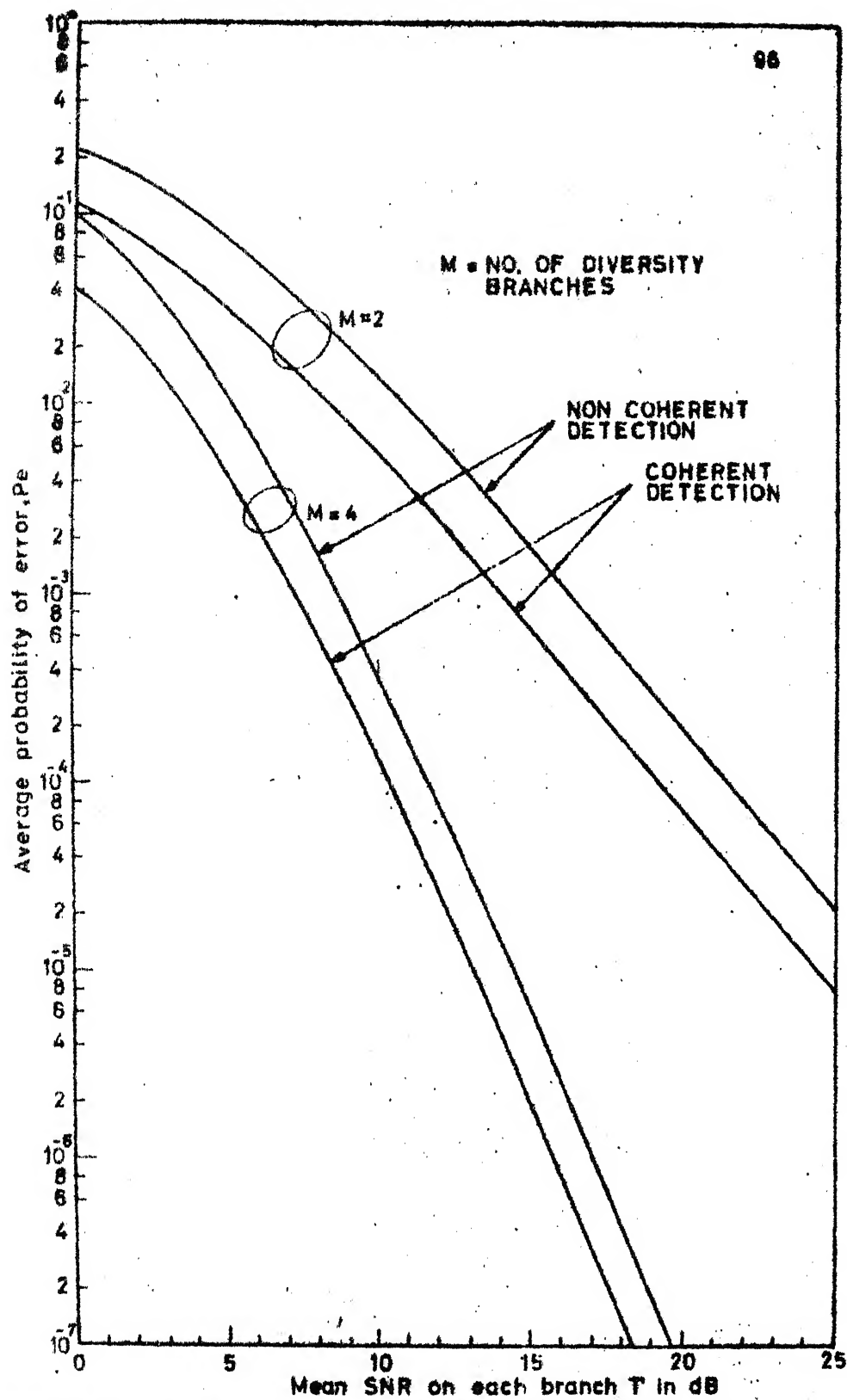


Fig.5-1 Performance of FSK under diversity

Thus

$$P_e = \int_0^{\infty} \frac{1}{2} \operatorname{erfc}(\sqrt{\gamma/2}) p(\gamma) d\gamma \quad (5.2.2)$$

where $p(\gamma)$ is given by equation (5.1.4). A closed form evaluation of equation (5.2.25) is not possible. However the integral has been numerically evaluated for values of $M=2$ and 4.

Table 5.1 shows the results of numerical calculations where average probabilities of errors have been calculated for various SNRs for values of $M=2$ and 4. Graphs have been shown in Figure 5.1 between average probability of error (P_e) and mean SNR ($\bar{\gamma}$) of each diversity branch.

The SNRs per bit required to achieve bit error rates of 10^{-2} , 10^{-4} and 10^{-6} have been shown in Tables 5.7 and 5.8 for $M=2$ and 4 respectively.

5.2.2 BFSK: Envelope detection [5]

The conditional probability of error is given here by equation (2.3.3) as

$$P_e(\gamma) = \frac{1}{2} e^{-\gamma/2} \quad (5.2.3)$$

Therefore the average probability of error is given by

$$P_e = \int_0^{\infty} \frac{1}{2} e^{-\gamma/2} p(\gamma) d\gamma \quad (5.2.4)$$

Table 5.2

Probabilities of errors at various SNRs for FSK:

Non-coherent detection

SNR Γ (dB)	Probability of error, P_e	
	No. of diversity branches (M)=2	No. of diversity branches (M)=4
0	2.222×10^{-1}	9.876×10^{-2}
2	1.556×10^{-1}	4.843×10^{-2}
4	9.824×10^{-2}	1.930×10^{-2}
6	5.590×10^{-2}	6.251×10^{-3}
8	2.896×10^{-2}	1.677×10^{-3}
10	1.388×10^{-2}	3.858×10^{-4}
12	6.277×10^{-3}	7.882×10^{-5}
14	2.719×10^{-3}	1.479×10^{-5}
16	1.144×10^{-3}	2.617×10^{-6}
18	4.719×10^{-4}	4.455×10^{-7}
20	1.922×10^{-4}	7.390×10^{-8}
22	7.764×10^{-5}	1.205×10^{-8}
24	3.119×10^{-5}	1.946×10^{-9}
25	1.974×10^{-5}	7.800×10^{-10}

Substituting the value of $p(\gamma)$ from equation (5.1.4) into equation (5.2.4) and solving, we get

$$P_e = \frac{1}{2} \frac{1}{\left(1 + \frac{\Gamma}{2}\right)^M} \quad (5.2.5)$$

Table 5.2 shows the results of numerical calculations for values of $M=2$ and 4 where probabilities of errors have been calculated for various values of mean SNR (Γ). Graphs have been shown in Fig. 5.1 between P_e and Γ for values of $M=2$ and 4.

The SNRs per bit required ^{to} achieve bit error rates of 10^{-2} , 10^{-4} and 10^{-6} have been shown in Tables 5.7 and 5.8 for $M=2$ and 4 respectively.

5.3.1 BPSK: Ideal coherent detection [5]

In this case, the conditional probability of error is given by equation (2.4.2) as

$$P_e(\gamma) = \frac{1}{2} \operatorname{erfc}(\sqrt{\gamma}) \quad (5.3.1)$$

Hence the average probability of error is given as

$$P_e = \int_0^{\infty} \frac{1}{2} \operatorname{erfc}(\sqrt{\gamma}) p(\gamma) \gamma \quad (5.3.2)$$

where $p(\gamma)$ is given by equation (5.1.4).

Table 5.3

Probabilities of errors at various SNRs for

Differential PSK

SNR Γ (dB)	Probability of error, P_e	
	No. of diversity branches (M)=2	No. of diversity branches (M)=4
0	1.250×10^{-1}	3.125×10^{-2}
2	7.483×10^{-2}	1.119×10^{-2}
4	4.054×10^{-2}	3.287×10^{-3}
6	2.015×10^{-2}	8.122×10^{-4}
8	9.358×10^{-3}	1.751×10^{-4}
10	4.132×10^{-3}	3.415×10^{-5}
12	1.761×10^{-3}	6.204×10^{-6}
14	7.329×10^{-4}	1.074×10^{-6}
16	3.002×10^{-4}	1.802×10^{-7}
18	1.217×10^{-4}	2.962×10^{-8}
20	4.901×10^{-5}	4.804×10^{-9}
22	1.965×10^{-5}	7.727×10^{-10}
24	7.861×10^{-6}	1.236×10^{-10}
25	4.968×10^{-6}	4.937×10^{-11}

Equation (5.3.2) is essentially same as equation (5.2.2) except that γ is modified here by a factor of 2. As such results obtained for BFSK coherent scheme will be obtained here also but at 3 dB lower values of r .

The values of bit SNRs required to achieve bit error rates of 10^{-2} , 10^{-4} and 10^{-6} have been shown in Tables 5.7 and 5.8 to be exactly 3dB lesser than that of BFSK coherent scheme.

5.3.2 DPSK [5]

The conditional probability of error is given here by equation (2.4.3) as

$$P_e(\gamma) = \frac{1}{2} e^{-\gamma} \quad (5.3.3)$$

The average probability of error is therefore, given as

$$P_e = \int_0^{\infty} \frac{1}{2} e^{-\gamma} p(\gamma) d\gamma \quad (5.3.4)$$

Solving equation (5.3.4) by substituting the value of $p(\gamma)$ from equation (5.1.4) yields

$$P_e = \frac{1}{2} \frac{1}{(1+F)^M} \quad (5.3.5)$$

Table 5.3 shows the results of numerical calculations where values of P_e have been calculated at various values of

γ for $M = 2$ and 4. A comparison of Tables 5.2 and 5.3 shows that DPSK gives a 3 dB better performance than BFSK non-coherent scheme.

The SNRs per bit required to achieve bit error rates of 10^{-2} , 10^{-4} and 10^{-6} have been shown in Tables 5.7 and 5.8 for $M=2$ and 4 respectively.

5.4 OOK: Coherent detection [5]

The conditional probability of error, here, is given by equation (2.2.4) as

$$P_e(\gamma) = \frac{1}{2} \operatorname{erfc} \left(\frac{\sqrt{\gamma}}{2} \right) \quad (5.4.1)$$

Hence the average of probability of error is given by

$$P_e = \int_0^{\infty} \frac{1}{2} \operatorname{erfc} \left(\frac{\sqrt{\gamma}}{2} \right) p(\gamma) d\gamma \quad (5.4.2)$$

Equations (5.4.2) and (5.2.2) are essentially same except that γ has been modified here by a factor of 1/2. As such results obtained for BFSK coherent scheme will be achieved here also but at 3 dB higher values of average mean SNR ($\bar{\gamma}$).

The SNRs per bit required to achieve bit error rates of 10^{-2} , 10^{-4} and 10^{-6} have been shown in Tables 5.7 and 5.8 for values of $M=2$ and 4 respectively.

5.5 Multiphase PSK: Coherent detection

The expression for conditional probability of error given by equation (3.3.4) in case of multiphase PSK is very complicated in itself. To use this for calculating the average probability of error by multiplying it with the value of $p(\gamma)$ given by equation (5.1.4) and then integrating the resultant expression over the entire range of $\gamma(0, \infty)$, does not seem to be mathematically viable for closed form expression. However a simple but approximate formula for conditional probability of error for L-phase PSK is known which can be used to calculate the average probability of error. The approximate conditional probability of error is given by Eqn. (2.5.13) which is quite accurate for values of $L \geq 4$. As, a simple but exact expression for conditional probability of error given by equation (2.5.15) in case of 4-phase PSK (QPSK) is known, we can use this expression for calculating the average probability of error. Thus errors figure only in case of $L=8$ and 16 . But at these values of L , errors are insignificant for our purposes as the expression given by equation (2.5.13) is quite accurate for these values of L .

4-phase PSK (QPSK)

The conditional probability of error is given by equation (2.5.15) as

Table 5.4

Probabilities of errors at various SNRs for QPSK

SNR r (dB)	Probability of error, P_e	
	No. of diversity branches (M)=2	No. of diversity branches (M)=4
0	2.077×10^{-1}	7.819×10^{-2}
2	1.380×10^{-1}	4.142×10^{-2}
4	8.273×10^{-2}	1.509×10^{-2}
6	4.497×10^{-2}	4.380×10^{-3}
8	2.243×10^{-2}	1.170×10^{-3}
10	1.044×10^{-2}	2.648×10^{-4}
12	4.620×10^{-3}	5.293×10^{-5}
14	1.971×10^{-3}	9.748×10^{-6}
16	8.207×10^{-4}	1.701×10^{-6}
18	3.362×10^{-4}	2.869×10^{-7}
20	1.363×10^{-4}	4.729×10^{-8}
22	5.492×10^{-5}	7.685×10^{-9}
24	2.202×10^{-5}	1.237×10^{-9}
26	8.810×10^{-6}	-
28	3.517×10^{-6}	-
30	1.403×10^{-6}	-

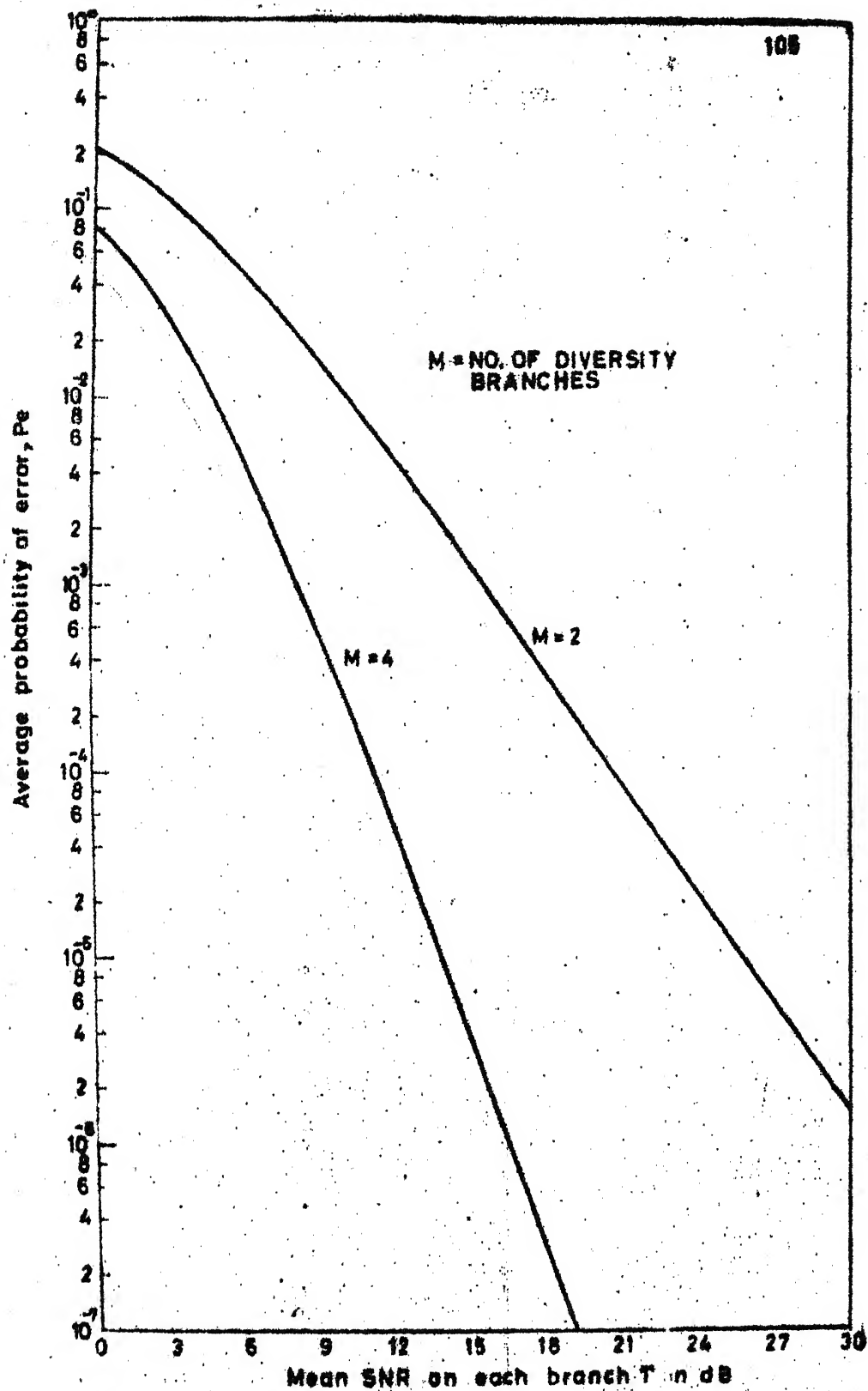


Fig.5-2 Performance of QPSK under diversity

$$P_e(\gamma) = \text{erfc}(\sqrt{\gamma}/2) \left[1 - \frac{1}{4} \text{erfc}(\sqrt{\gamma}/2) \right] \quad (5.5.1)$$

Therefore the average probability of error is given by

$$P_e = \int_0^{\infty} P_e(\gamma) p(\gamma) d\gamma \quad (5.5.2)$$

where $p(\gamma)$ is given by equation (5.1.4).

Table 5.4 shows the results of numerical calculations where symbol error probabilities have been calculated for various values of symbol SNRs for values of $M=2$ and 4. Graphs have been plotted between P_e and $\bar{\gamma}$ for values of $M=2$ and 4 and shown in Figure 5.2.

Tables 5.7 and 5.8 show the values of SNRs per bit required to achieve bit error rates of 10^{-2} , 10^{-4} and 10^{-6} for $M=2$ and $M=4$ respectively.

8 and 16-phase PSK:

The conditional probability of error, here, is given by equation (2.5.13) as

$$P_e(\gamma) = \text{erfc}(\sqrt{\gamma} \sin \pi/L) \quad (5.5.3)$$

Therefore the average probability of error is given by

$$P_e = \int_0^{\infty} \text{erfc}(\sqrt{\gamma} \sin \pi/L) p(\gamma) d\gamma \quad (5.5.4)$$

Table 5.5

Probabilities of errors at various SNRs for 8-phase PSK

SNR Γ (dB)	Probability of error, P_e	
	No. of diversity branches (M)=2	No. of diversity branches (M)=4
6	1.920×10^{-1}	7.082×10^{-2}
8	1.240×10^{-1}	2.756×10^{-2}
10	7.178×10^{-2}	9.162×10^{-3}
12	3.779×10^{-2}	2.585×10^{-3}
14	1.838×10^{-2}	6.255×10^{-4}
16	8.410×10^{-3}	1.332×10^{-4}
18	3.675×10^{-3}	2.581×10^{-5}
20	1.555×10^{-3}	4.669×10^{-6}
22	6.445×10^{-4}	8.066×10^{-7}
24	2.632×10^{-4}	1.351×10^{-7}
26	1.065×10^{-4}	2.218×10^{-8}
28	4.284×10^{-5}	3.596×10^{-9}
30	1.716×10^{-5}	5.781×10^{-10}

Table 5.6

Probabilities of errors at various SNRs for
16-phase PSK

SNR Γ (dB)	Probability of error, P_e	
	No. of diversity branches (M)=2	No. of diversity branches (M)=4
6	-	3.616×10^{-1}
8	-	2.390×10^{-1}
10	2.514×10^{-1}	1.358×10^{-1}
12	1.856×10^{-1}	6.201×10^{-2}
14	1.192×10^{-1}	2.462×10^{-2}
16	6.855×10^{-2}	8.276×10^{-3}
18	3.588×10^{-2}	2.330×10^{-3}
20	1.737×10^{-2}	5.598×10^{-4}
22	7.918×10^{-3}	1.184×10^{-4}
24	3.451×10^{-3}	2.280×10^{-5}
26	1.458×10^{-3}	4.107×10^{-6}
28	6.034×10^{-4}	7.075×10^{-7}
30	2.462×10^{-4}	1.182×10^{-7}
32	9.960×10^{-5}	-
34	4.005×10^{-5}	-
36	1.604×10^{-5}	-
38	6.414×10^{-6}	
40	2.560×10^{-6}	

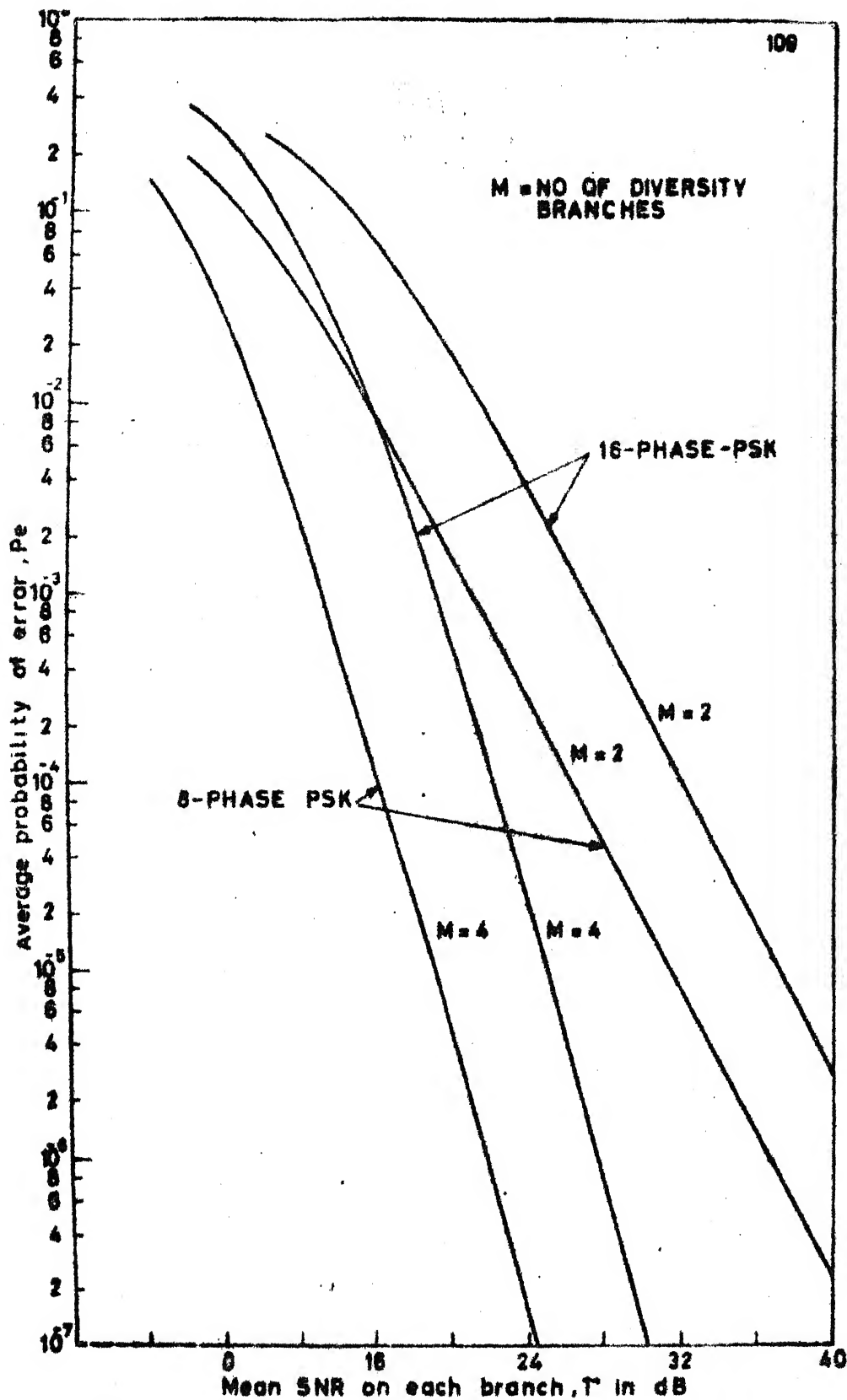


Fig. 5.3 Performance of multi-phase coherent PSK under diversity

where $p(\gamma)$ is given by equation (5.1.4).

Tables 5.5 and 5.6 show the results of numerical calculations where average probabilities of errors have been calculated for various values of symbol SNRs (Γ) at values of $M=2$ and 4 for 8 and 16 phase PSK respectively. Graphs have been shown in Figure 5.3 between P_e and Γ for 8 and 16 phase PSK at $M=2$ and 4.

Tables 5.7 and 5.8 show the values of SNRs per bit required to achieve bit error rates of 10^{-2} , 10^{-4} and 10^{-6} for values of $M=2$ and 4 respectively.

The criterion used to convert symbol error rates to bit error rates and symbol SNRs to bit SNRs for multiphase PSK here also has been assumed to be same as in Chapter 2.

5.6 MSK and OK-QPSK:

Under the assumptions of coherent detection and assumptions made in Chapter 2 Section 2.6, the conditional bit error rate for MSK and OK-QPSK is same as BPSK coherent detection. Therefore the average probability of error will be same for these two system as BPSK.

5.7 Comparison of various digital systems under linear diversity combining techniques:

Tables 5.7 and 5.8 have been prepared to portray the performances of various digital modulation schemes under

Table 5.7

Performance of representative digital modulation schemes under maximal ratio combining

Modulation schemes	Average mean SNR ($\bar{\gamma}$) in dB No. of diversity branches (M) = 2		
	$P_e=10^{-2}$	$P_e=10^{-4}$	$P_e=10^{-8}$
OOK: coherent detection	8.4	19.2	29.6
FSK: coherent detection	8.4	19.2	29.6
FSK: Non-coherent detection	10.8	21.4	31.5
BPSK	5.4	16.2	26.3
DPSK	7.8	18.4	28.5
MSK ($h = .5$)	5.4	16.2	26.3
OK-QPSK	5.4	16.2	26.3
QPSK	5.4	16.2	26.3
8-PSK	7.93	19.03	29.23
16-PSK	11.68	22.98	32.98

Table 5.8

Performance of representative digital modulation
schemes under maximal ratio combining

Modulation schemes	Average mean SNR (Γ) in dB No. of diversity branches (M) = 4		
	$P_e=10^{-2}$	$P_e=10^{-4}$	$P_e=10^{-6}$
OOK: coherent detection	3.5	10.35	15.75
FSK: coherent detection	3.5	10.35	15.75
FSK: Non-coherent detection	5.2	11.7	17.1
BPSK	0.5	7.3	12.75
DPSK	2.2	8.7	14.1
MSK($h = .5$)	0.5	7.3	12.75
OK-QPSK	0.5	7.3	12.75
QPSK	0.6	7.35	12.75
8-PSK	3.03	10.13	15.73
16-PSK	6.98	14.38	19.98

maximal ratio combining technique with dual and quadrature diversities. SNRs per bit required to achieve BERs of 10^{-2} , 10^{-4} and 10^{-6} have been shown in these tables for the systems earlier discussed.

A comparison of tables 4.2 and 5.7 shows that there is a considerable improvement in the performances of various systems even with dual diversity as compared to Rayleigh fading signals without diversity. The advantage gained in terms of \angle SNR is greater than 7 dB at $P_e = 10^{-2}$ and 16 dB at $P_e = 10^{-4}$.

A similar comparison of Tables 4.2 and 5.8 shows a tremendous improvement in the performances of various systems with quadrature diversity. Here the advantage gained in terms of SNR is greater than 12 dB at $P_e = 10^{-2}$ and 24 dB at $P_e = 10^{-4}$.

Therefore it is seen that by increasing the number of diversity branches, the performance of systems can be improved tremendously. But one cannot increase the number of diversity branches without increasing the complexity of receiver with the constraint of economic viability.

We have assumed for our calculations that all the branch signals are uncorrelated and maximal ratio combining

is optimum. However, in practice, it is not possible to achieve either uncorrelated branch signals or optimal maximal ratio combining. So if we take into account these factors, the performance of systems shown in Tables 5.7 and 5.8 will degrade. It has been shown that performance of a system even with dual diversity is better than no diversity system even if the cross-correlation coefficient of signals on the two branches is of the order of 0.99 [20]. Therefore it can be concluded that diversity is a very effective method of combating the effect of fading.

CHAPTER 6

CONCLUSIONS

We have studied the performance of various digital modulation techniques under ideal conditions in Chapter 2. SNR required to achieve various BERs have been shown in Table 2.4. In Chapter 3, communication efficiency as measured by data rate per unit bandwidth has been compared for various systems, again under ideal conditions. In Chapter 4, the effect of Rayleigh fading on the performance of these techniques has been studied. Table 4.2 shows that Rayleigh fading causes severe degradation on the performance of various digital modulation techniques. To overcome the effect of Rayleigh fading, linear diversity combining techniques have been studied in Chapter 5.

The performance of a digital modulation technique must be adjudged taking into account many factors which affect the performance of the scheme. Some of these important factors are ISI due to channel and receiving filters, co-channel and adjacent channel interferences, fading and phase jitter introduced by the channel. Also the channel may not be always Gaussian but may be impulsive in nature e.g. the telephone channel. Since we have discussed

the performance of various digital modulation techniques under ideal conditions and subsequently under Rayleigh fading, our conclusions are based on these studies only. However, after allowing for various factors mentioned above, the relative performance will not change significantly. The performance may be obtained by allowing degradation caused by the above mentioned factors.

If one chooses to make minimum probability of error as performance criterion, then looking at Table 2.4, the obvious choice is CPFSK($h=0.75$) coherent detection scheme with 3 or 5 bits observation intervals. Although, theoretical this scheme provides the best possible performance under ideal conditions, the practical implementation of this scheme is a very difficult task. This is due mainly to two factors. Firstly, it is impossible to achieve an exact phase reference at the receiver for coherent detection of the CPFSK waveform. Secondly, the scheme involves a very complex instrumentation. Therefore, the advantage gained in terms of transmitted power may be lost in terms of complexity and cost of the receiver. At high SNR operation, the above problem can be overcome by non-coherent detection of CPFSK waveform with 5 bits observation interval. This scheme outperforms coherent BPSK scheme above 8 dB (approx.)

of SNR. Also, this scheme does not require phase reference at the receiver and hence is relatively simple to implement. QPSK, OK-QPSK and MSK ($h=0.5$) are other schemes which give next best performances. These schemes have an advantage in that they exhibit a relatively good data rate per unit bandwidth (R/B) performance.

If one wants to make the data rate per unit bandwidth (R/B) as performance criterion, then SSB-SC AM gives the best performance followed by coherent M-ary PSK schemes (8 and 16 PSK). For both these schemes, to retain the same R/B, one must increase the required SNR if probability of error is to be decreased. Although SSB-SC AM provides best R/B performance, its performance as regards to minimising the probability of error is not as good as other equivalent techniques. Similarly, although coherent M-ary PSK gives a very good R/B performance, it is one of the most complex systems to implement. As a compromise between performance and complexity of the receiver, MSK, QPSK and OK-QPSK are systems which give a good R/B performance. Among these, OK-QPSK has the advantage of neutralising the effect of ISI to a great extent.

Table 2.4 represents simply a weighted average of ideal performance values. Therefore, the relative performance

of schemes does not differ markedly from that shown in Table 2.4. Table 4.2 shows that there is severe degradation in the performance of these schemes under Rayleigh fading signals as compared to non-fading signals. The degradation is in terms of tens of decibels of additional SNR required to maintain the same BER e.g. an additional SNR of 25.6 dB at $P_e=10^{-4}$. Our earlier discussions hold good here also regarding the selection of a particular scheme for a particular purpose.

To overcome the effect of fading, linear diversity combining techniques are utilised. Table 5.7 and 5.8 portray the performance of the various digital modulation techniques under dual and quadrature diversities respectively. It is seen that by increasing the number of diversity branches, the performance of a system can be improved tremendously. But one cannot increase the number of diversity branches without increasing the complexity of the receiver and economic viability. The relative performance of the schemes remain same as that indicated in Table 2.4. Thus, while selecting number of diversity branches, one has to make compromise between the performance and the complexity of the receiver.

In general, it is difficult to evaluate the cost of a particular scheme without conducting a full scale investigation of the cost and complexity tradeoffs with many alternate implementation options. Nevertheless, modulation methods can be ranked according to their inherent complexity and results of such ranking are shown in Figure 6.1.

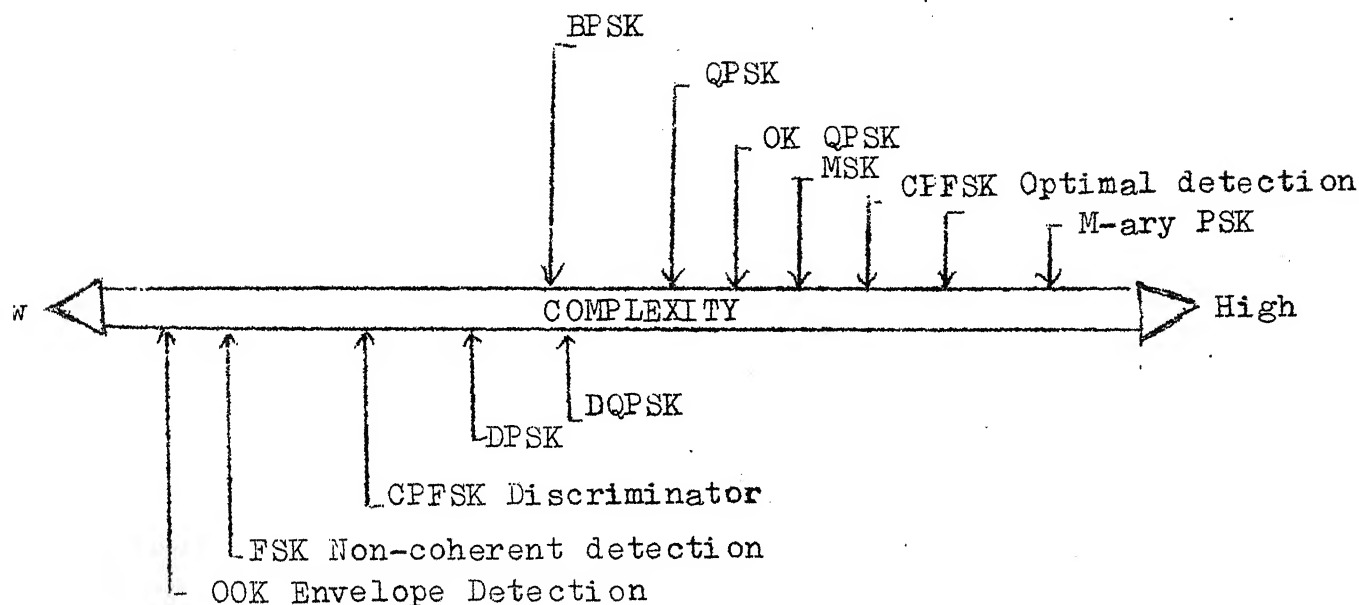


Fig. 6.1 Relative Complexity of Representative Modulation Schemes

In our study, we have not considered the effects due to ISI, phase jitter, cochannel, and adjacent channel interferences on the performance of various systems. It may be desirable to evaluate the system performance under the

influence of above factors. One can also study the effect of delay distortion caused by the channel. Due to the paucity of time, we have also not studied some of the digital techniques such as QPR (Quadrature partial response) QAM (quadrature amplitude modulation) and APK (Amplitude phase modulation techniques). These may constitute the basis for further study.

REFERENCES

1. S. Stein and J.J. Jones, "Modern Communication Principles": Mc-Graw Hill, 1967, New York.
2. R.W. Lucky, J. Salz, and E.J. Weldon, "Principles of data communication": Mc-Graw Hill, 1968, New York.
3. J.M. Wozencraff and I.M. Jacobs, "Principles of Communication Engineering": Wiley, 1965, New York.
4. H.L. Vantrees, "Detection, Estimation and Modulation Theory Part I": Wiley, 1968, New York.
5. M. Schwartz, W. Bennet and S. Stein, "Communication System and Technique": Mc-Graw Hill, 1966, New York.
6. T.A. Schonhoff, "Symbol Error Probabilities for M-ary CP-FSK coherent and non-coherent detection", IEEE Transaction on Communication, vol. COM-24, June 1976, pp. 644-652.
7. S.A. Gronemeyer and A.L. Mcbridge, "MSK and offset QPSK Modulation" IEEE Transactions on Communication, vol. COM-24, Aug. 1976, pp. 809-82.
8. H.C. Salwan and C.B. Duncombe, "Performance Evaluation of Data Modems for the Aeronautical Satellite Channel", IEEE Transactions on Communication, vol. COM-23, July 1975, pp. 695-705.
9. S.Y. Kwon and N.M. Shehadeh, "Analysis of incoherent Frequency Shift-keyed Systems", IEEE Transactions on Communication, vol. COM-23, Nov. 1975, pp. 1331-1339.
10. M.C. Austin, "Wide band Frequency Shift-keyed Receiver Performance in the presence of the Inter-symbol Inter-ferece" IEEE Transactions on Communications, vol. COM-23, April 1975, pp. 453-459.
11. R.C. Harper, "Adaptive Phase and Amplitude Modulation on a Frequency Dispersive Fading Channel", IEEE Transactions on Communication, vol. COM-22, June 1974, pp. 764-776.
12. W.P. Osborne and M.B. Lunz, "Coherent and Non-coherent Detection of CP-FSK", IEEE Transactions on Communication, vol. COM-22, Aug. 1974, pp. 1023-1036.
13. R.De.Buda, "About Optimal Properties of Fast-Frequency-Shift-Keying", IEEE Transactions on Communication, vol. COM-22, Oct. 1974, pp. 1726-1727.

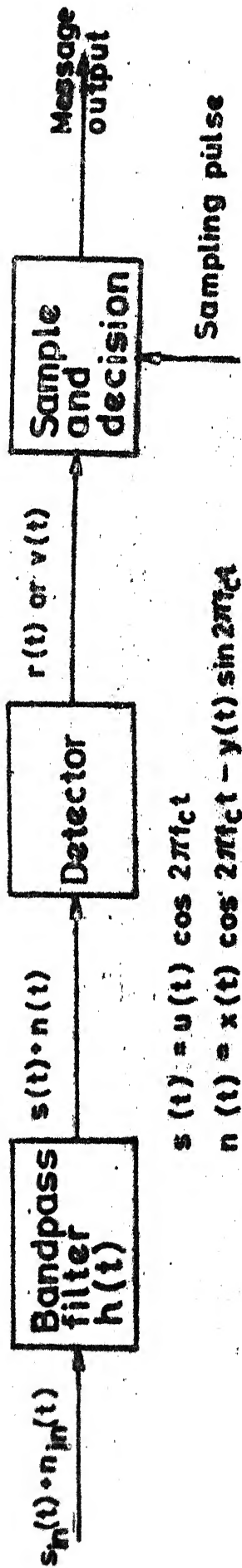
14. S.A. Rhodes, "Effect of Noisy Phase Reference on Coherent Detection of Offset-QPSK Signals", IEEE Transactions on Communication, vol. COM-22, Aug. 1974, pp. 1046-1055.
15. V.K. Prabhu, "Error Probability Performance of M-ary CPSK Systems with Intersymbol Interference", IEEE Transactions on Communication, vol. COM-21, Feb. 1973, pp. 99-109.
16. M.K. Simon "An MSK Approach to Offset QPSK", IEEE Transactions on Communication, vol. COM-24, Aug. 1976, pp. 921-923.
17. J.J. Jones, "Multichannel FSK and DPSK Reception with three Component Multipath": IEEE Transactions on Communication, vol. COM-16, Dec. 1968, pp. 808-821.
18. W.R. Bennet and J.R. Davey, "Data Transmission": McGraw Hill, 1965, New York.
19. P.A. Kullotam, "Differentially Coherent Demodulation of BPSK and QPSK Signals in Presence of Doppler and Noise", Proceeding of National Telecommunication Conference, 1974, pp. 221-227.
20. Yiyagaki, N. Morianga and T. Mamekawa, "Error Probability of CPSK Signals through m-distributed fading channel", IEEE Transactions on Communication, vol. COM-26, Jan. 1978, pp. 88-100.
21. A.R. DiDonato and M.P. Jarnagin, "A method for computing the circular coverage functions": Mathematics of Computation, vol. 16, pp July 1962, pp. 347-355.
22. A.B. Carlson, "An introduction to signals and noise in electrical communications", McGraw Hill, 1968, Tokyo.
23. Jack Satz, "Communication efficiency of digital modulation systems", IEEE Transactions on Communication, vol. COM-18, April 1970, pp. 97-102.
24. R. De Buda, "Coherent demodulation of Frequency Shift-Keying with low deviation ratio"; IEEE Transactions on Communication, vol. COM-20, June 1972, pp. 429-435(Part I).
25. C.R. Cahn, "Performance of Digital Phase Modulation Communication Systems", IRE Trans. Communication System, CS-7 pp. 3-6, 1959 (May).
26. G.J. Garrison, "A power spectral density analysis for digital FM", IEEE Transactions on Communication, vol. COM-22, Nov. 1975, pp. 1228-1243.

```

00100      C                               APPENDIX A
00200      C      THIS PROGRAMME CALCULATES MARCUM Q FUNCTION
00300      C      R*D SHOULD BE SMALLER THAN 30
00400      C      PROGRAMME GIVES ACCURATE RESULT UPTO 1E-7
00500      C      SUBROUTINE MARCUM(R,D,Q)
00600      C      DIMENSION S(400),T(400)
00700      C      SUM1=0.0
00800      C      SUM2=0.0
00900      C      EPS=0.1E-10
01000      C      N=1
01100      C      S(2)=EXP(-(R**2+D**2)/2.0)
01200      C      T(2)=ABS(R**2-D**2)/(R**2+D**2)*(1.0-S(2))
01300      C      N=N+1
01400      C      I=2*N; AN=N-1
01500      C      S(I)=((R*D/(2.0*AN))**2)*S(I-2)
01600      C      A=((2.0*AN-1.0)/(2.0*AN)
01700      C      B=((2.0*R*D/(R**2+D**2))**2)*T(I-2)
01800      C      C=ABS(R**2-D**2)/(R**2+D**2)
01900      C      E=(1.0+(4.0*AN/(R**2+D**2)))*S(I)
02000      C      T(I)=A*B-C*E
02100      C      SUM1=SUM1+0.5*(1.0-S(I)+T(I))
02200      C      SUM2=SUM2+0.5*(1.0-S(I)-T(I))
02300      C      IF((S(I).GT.EPS).AND.(T(I).GT.EPS)) GO TO 30
02400      C      IF(N.EQ.400) GO TO 60
02500      C      GO TO 2
02600      C      IF(R.GT.0) GO TO 75
02700      C      PRD=SUM2-S(2)/2.0-T(2)/2.0
02800      C      GO TO 76
02900      C      PRD=SUM1-S(2)/2.0+T(2)/2.0
03000      C      76 Q=1.0-PRD
03100      C      Q(D,R)=1-P(R,D)
03200      C      GO TO 70
03300      C      60 TYPE 100
03400      C      100 FORMAT(10X,'DOES NOT CONVERGE')
03500      C      70 RETURN
03600      C      END

```

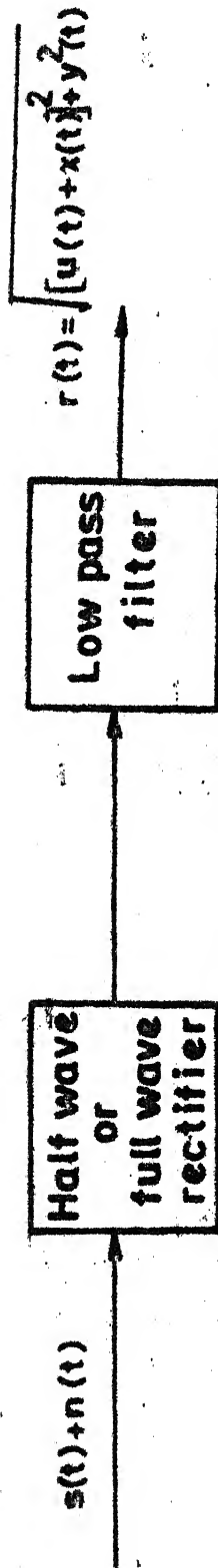
APPENDIX B1



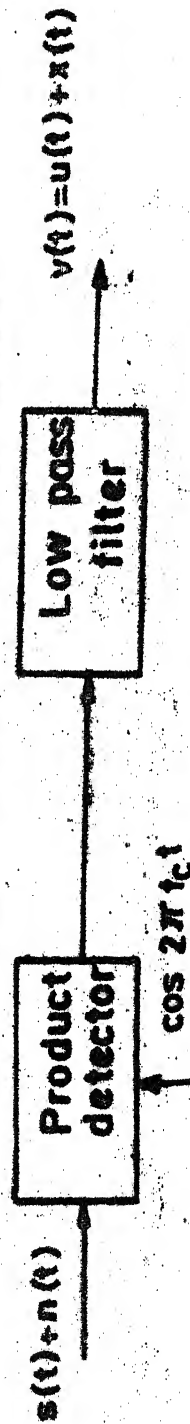
$$s(t) = u(t) \cos 2\pi f_c t$$

$$n(t) = x(t) \cos 2\pi f_c t - y(t) \sin 2\pi f_c t$$

(a) Elements of a simple receiver

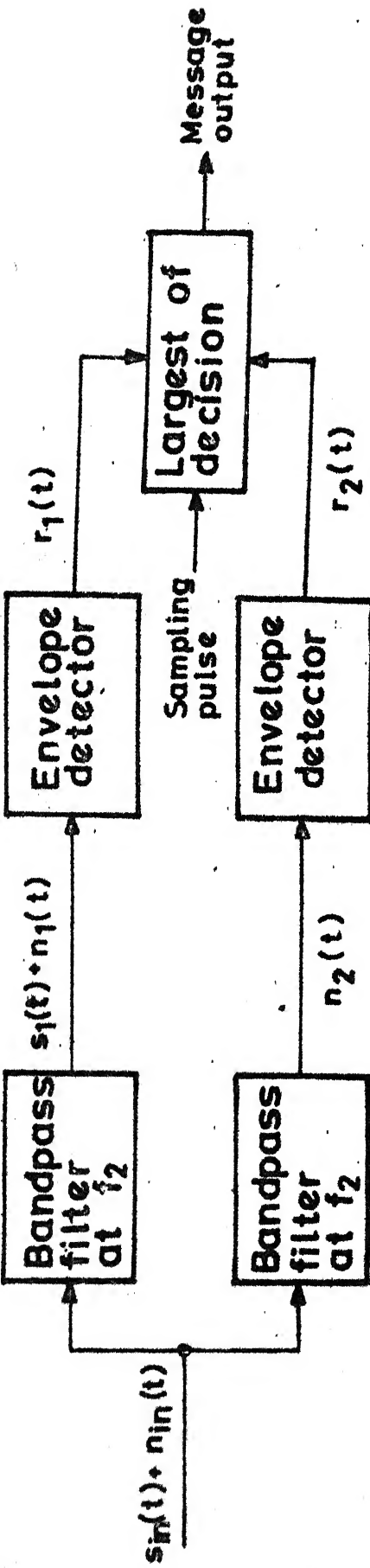


(b) Noncoherent (envelope) detector

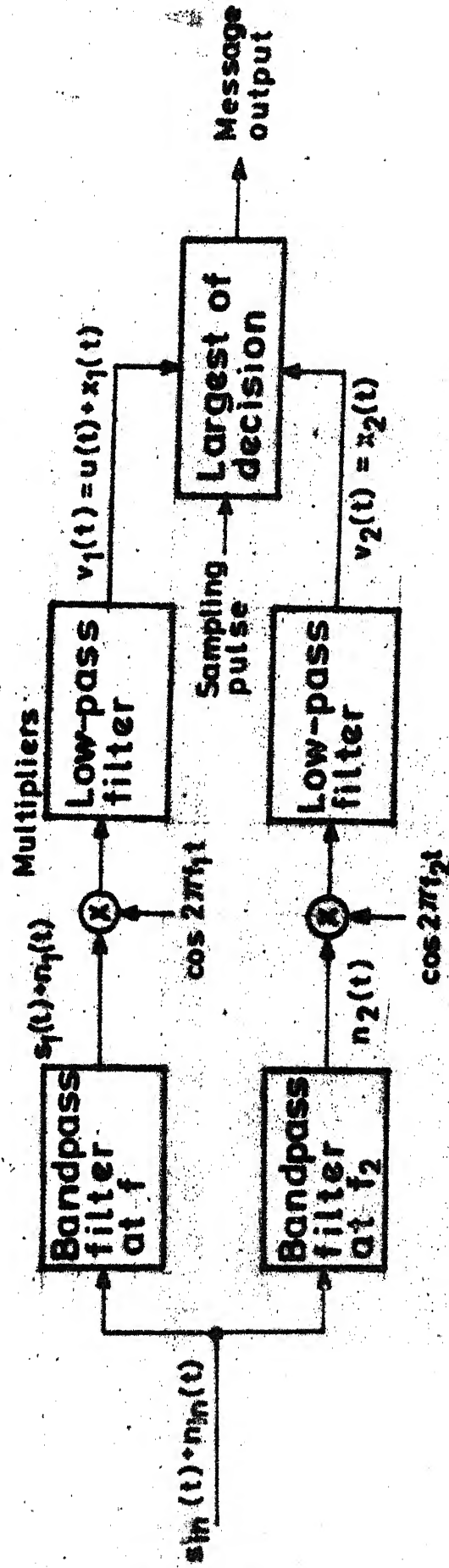


(c) Coherent (synchronous) detector

Elements of a binary digital receiver (OOK)



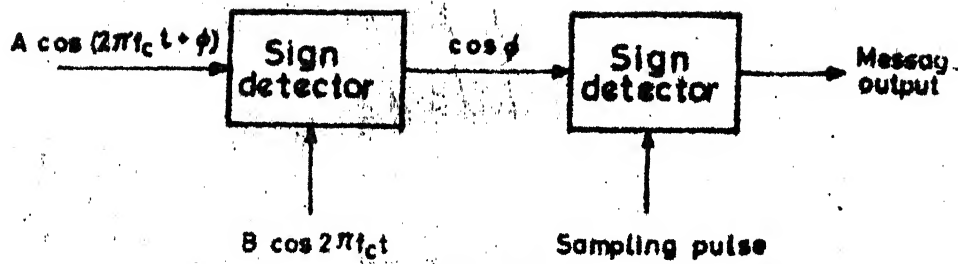
(a) Noncoherent detection tone f_1 signaled



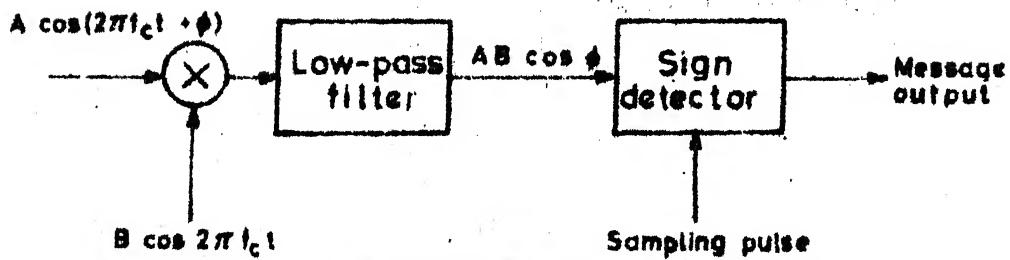
(b) Coherent detection, tone f_1 signaled

Dual-filter detection of binary FSK signals

B3

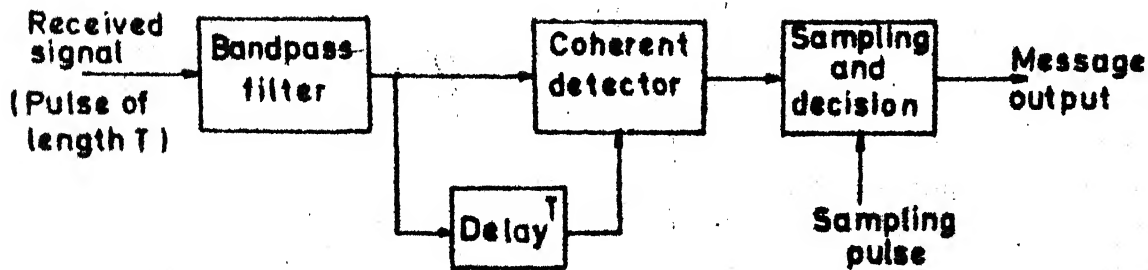


(a) Phase detection



(b) Coherent detection

Two detection schemes for ideal coherent PSK



Differentially coherent phase shift keying